Article

Heterojunction Technology vs. Passivated Emitter and Rear Contact Photovoltaic Panels: Evaluating Efficiency and Profitability Under Challenging Summer Conditions in Lisbon Using Extensive Field Data

André Sapina [1] and Paulo Branco [2,*]

[1] Instituto Superior Técnico, University of Lisboa, 1049-001 Lisboa, Portugal; andresapina@tecnico.ulisboa.pt
[2] IDMEC, Instituto Superior Técnico, University of Lisboa, 1049-001 Lisboa, Portugal
* Correspondence: pbranco@tecnico.ulisboa.pt

Abstract: Renewable energy is essential for reducing fossil fuel dependence and achieving carbon neutrality by 2050. This study compares the widely used passivated emitter and rear contact (PERC) cells with advanced heterojunction technology (HJT) cells. Conducted in Lisbon during August 2022, this research evaluates the energy yield of PV installations over 400 W under challenging summer conditions. HJT cells, which combine monocrystalline silicon and amorphous layers, showed a 1.88% higher efficiency and a 3% to 6% increase in energy yield compared to PERC cells. This study also examines the effects of irradiance and temperature on performance using experiment field data. HJT modules are ideal for limited space or power constraints, offering long-term profitability, while PERC modules are more cost-effective for budget-limited projects.

Keywords: passivated emitter and rear contact; heterojunction technology; PERC; HJT; photovoltaic

1. Introduction

The performance of a photovoltaic (PV) module is strongly dependent on ambient conditions (e.g., irradiation, ambient temperature, wind), which cause different power losses occurring in the solar cells. These losses are related to the increased cell temperature and are associated with the recombination effect. Therefore, each electron–hole pair that is not collected reduces the cell efficiency. Several technologies were improved in the past century and are currently used to lower the recombination losses and the temperature coefficient. In 2020, 85% of the market share was occupied by the passivated emitter and rear contact (PERC) technology [1] due to the low cost of manufacture and high efficiency. However, this photovoltaic cell displays a high-temperature coefficient and light-induced degradation (LID). As usual, the market is constantly looking for improvements in the technology used. Interest has then risen around the heterojunction (HJT) cell due to its lower temperature coefficient, lower recombination rates, and natural bi-facial nature.

Recently, as shown in [2], advances in passivation techniques and improvements in their optical performance have led PERC and HJT technologies to new efficiency levels of around 28%. However, their field tests need to be settled. Only since 2022 have field experiments been performed with PERC and HJT modules to test their energy performance. In [3], field tests were completed in Hainan, China, characterized by specific climate characteristics, such as hot and humid summers and mild winters. An extensive review of

PERC and HJT technologies has lately been presented in [4]. It shows that these bifacial technologies have advantages but for certain applications and conditions. Not only that, but the authors also call for attention to the very few field experiments being presented, including application scenarios used to verify their performance/costs during their lifetime. The work in [5] studies the performance of bifacial PV systems using a model approach that can be used for their optimized operation in a certain field environmental condition. The experimental validation of the proposed energy yield model was made on the roof of the authors' academic building. As also pointed out in [6], there is still a lack of analysis focusing on different application levels. It is important to recognize that all previous references point to the limited number of functioning installations and operational data as important topics for the current and future PERC and HJT technology.

1.1. PERC-Passivated Emitter and Rear Contact

From an optical perspective, the power output is directly related to the amount of incident light absorbed by the cell. Silicon nitride acts as an anti-reflection coating, allowing more light to penetrate the cell, resulting in superior efficiency.

Defects at the silicon surface are caused by the interruption of the crystal lattice periodicity, and, as a result, unpaired electrons appear. These are called dangling bonds and generate a high local recombination rate.

Minimizing surface recombination, i.e., passivation, is thus a prerequisite for achieving high-efficiency cells. This is achieved by combining two effective mechanisms: chemical passivation by intrinsic hydrogen and field-effect passivation via fixed insulator charges [7]. Due to the high refractive index and the superior surface passivation, silicon nitride layers are applied in silicon solar cells.

1.1.1. Al_2O_3-Based Rear Surface Passivation Scheme

Rear surface passivation was improved by introducing aluminum oxide as a charged dielectric. This innovation became the basic element of the industrial PERC (passivated emitter and rear contact) device.

Fixed negative charges present in the Al_2O_3 film attract holes to form an accumulation layer on p-type silicon [8]; this effect is illustrated in Figure 1. This positively charged layer results in a recombination decrease [8]. Also, the flow of electrons along the rear surface in the direction of the highly recombinative base contacts is suppressed. Due to these advantages, Al_2O_3 has a high potential for increasing solar cell efficiency [9].
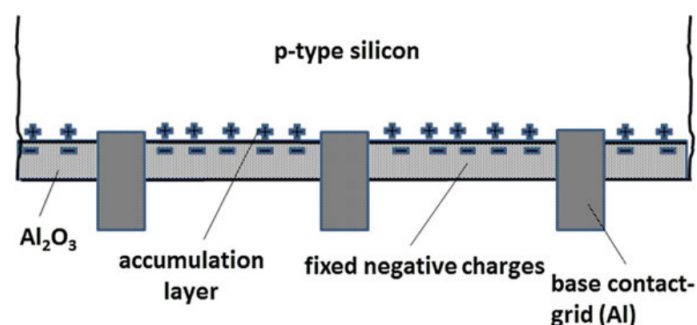
**Figure 1.** Rear surface passivation scheme illustrating the passivation layer located at the rear surface of the solar cell to reduce recombination losses and improve overall performance [8].

1.1.2. Al_2O_3/SiN_x-Stacks for PERC Solar Cells

When incident light is not absorbed, it reaches the back structure that supports the module, and energy is converted into heat, raising cell temperature and decreasing efficiency.

The combination of aluminum oxide and silicon nitrite provides passivation and creates a mirroring effect for incident light [10], enhancing its absorption within the solar cell. For these two mentioned reasons, combining these two layers on the back of the cell is fundamental to boosting the efficiency of photovoltaic cells. With a layer of silicon nitride on the front, the PERC cell is completed and is displayed in Figure 2.
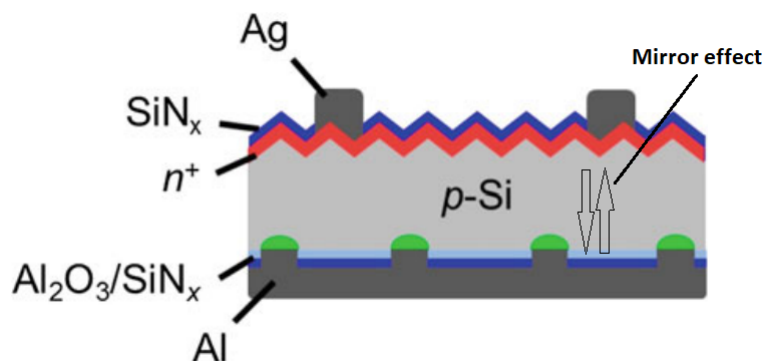

Figure 2. PERC cell scheme: 1—"Ag" composes the front electric contact; 2—"SiN_x" (silicon nitride) composes the anti-reflective coating. 3—"Al_2O_3" (aluminum oxide) forms the rear surface dielectric passivation layer; and the "Al" states a back surface increasing the electric field value to reduce the recombination.

Although some improvements were made and higher efficiency was achieved, this technology still presents light-induced degradation.

1.1.3. LID—Light-Induced Degradation

Besides challenges in process technology, stability issues due to light-induced degradation have been a critical challenge for highly efficient p-type solar cells. This LID can happen due to the boron–oxygen (BO) effect and light- and elevated-temperature-induced degradation (LeTID).

Under the light exposition effect, O_2 may diffuse across the silicon lattice and create complexes with boron acceptors. The boron–oxygen complexes create energy levels in the silicon lattice and can capture electrons and holes, which are lost for the PV effect. This effect happens when the panel is first exposed to sunlight, resulting in an instant decrease in efficiency, as seen in Figure 3.
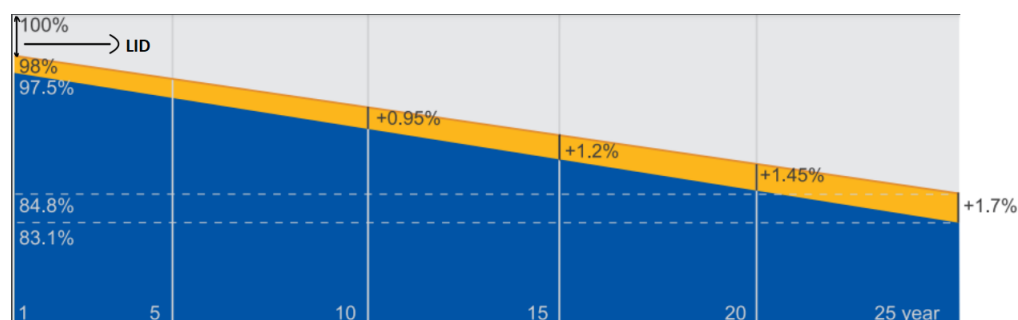
Figure 3. Efficiency decrease due to the light-induced degradation (LID).

The second process, as the name indicates, relates severe efficiency degradation with high temperature and, if not controlled, can lead to losses of more than 10% relative. Engineers have been trying to solve these inefficiency issues, and a solution was found. In contrast to conventional PERC, Hanwha Q CELLS' Q.ANTUM technology reliably suppresses both LID due to BO defect formation and LeTID in modules manufactured [11].

It is possible to conclude that, with the insertion of a silicon nitride anti-reflection coating on the front of the cell, the creation of passivation and a mirroring effect on the back, and the solution of LID-related inefficiencies, PERC is one of today's market competitors for high-efficiency mass production cells.

1.2. SHJ—Silicon Heterojunction Cell

As discussed in the previous paragraphs, high-efficiency solar cells can be obtained by implementing surface passivation layers that severely reduce recombination losses. This is achieved by the implementation of dielectric layers such as silicon nitride (SiN_x), silicon oxide (SiO_2), aluminum oxide (Al_2O_3) or intrinsic hydrogenated amorphous silicon.

The first three layers have already been described since some are applied to PERC cells. *Sanyo* invented heterojunction intrinsic thin-layer solar cell (HIT) technology in the early 1990s and benefited from using intrinsic hydrogenated amorphous silicon layers for higher efficiency. The concept of a diode using a heterojunction formed by amorphous silicon layers and crystalline silicon was initially proposed in 1974. However, it was only commercialized by *Sanyo* 18 years later. The term heterojunction comes from the formation of the junction of semiconductors with different bandgaps. This is verified in the cross-sectional view of SHJn in Figure 4, where an n-type silicon (c-Si(n)) is sandwiched between two amorphous silicon intrinsic layers (a-Si:H(i)).
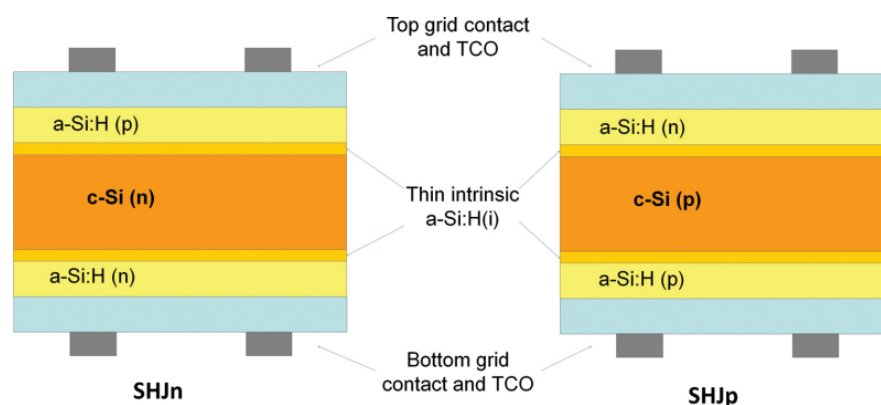
Figure 4. Cross-sectional view of SHJn (n-type and p-type silicon heterojunction). Both show an amorphous silicon layer (a-Si:H(i), i = p, n); a thin layer for surface passivation (a-Si:H(n)) for an n-type amorphous silicon layer [12].

Using the amorphous layers, surface recombination is suppressed by the chemical passivation of dangling bonds on the c-Si wafer surface. This is possible due to the formation of Si-Si and Si-H bonds [13]. Amorphous silicon layers only provide passivation if they are in contact with intrinsic layers. Intrinsic means that the layers have not been doped intentionally.

Continuing the analysis of the SHJn cell, displayed on the left part of Figure 4, a p-type amorphous layer (a-Si:H(p)) is grown on the top, and, on the bottom, n-type amorphous layers (a-Si:H(n)) are deposited. These layers are then fully covered with a transparent conductive oxide (TCO), followed by screen-printing contact metal grids using low-temperature Ag conductive paste. TCOs are required to enhance the collection of the electron–hole pair and are transparent to allow light to enter the cell.

Both n- and p-type doped wafers have been used for SHJ cells, but the highest efficiency was obtained for SHJn cells. It is important to note that the relation of a-Si/c-Si is roughly 1:10,000. From the studies conducted on these materials, n-type wafers display a lower recombination rate and lower sensitivity to metal impurities, and, unlike p-type, are not

affected by LID [14]. Adding to these advantages, SHJ cell assembly is performed at low temperatures (<250 °C), favoring thin wafers for cell production.

Sanyo commercialized this technology under the patented heterojunction with intrinsic thin layer (HIT). This patent expired in 2010 and opened the way for equipment suppliers and manufacturers to work with the technology and provide solutions to the market. *MeyerBurger* is a Swiss company that used to manufacture machinery required to produce wafers in mass production. After 2010, they started working on the heterojunction technology, and are present today with HJT + SmartWire Connection Technology (SWCT). It consists of a small wire to replace busbars on the top and bottom grid of the cell, as seen in Figure 5. This technology can increase the efficiency of the HJT cell by 5.7% due to the reduced electrical losses and optical losses (less shading) due to the reduced size compared to the bus bar technology [15].
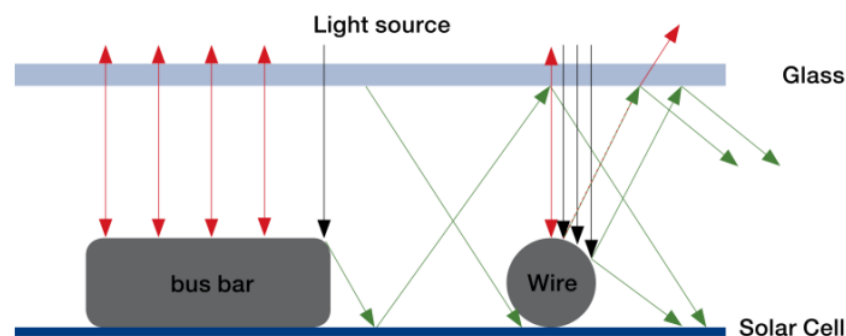
Figure 5. Busbar and SmartWire Connection Technology (SWCT): this decreases the amount of silver compared to busbar technology, also increasing the efficiency since it allows for reducing the shading effect and the series resistance of the cell. However, despite its higher initial costs, a reduction in silver usage can lead to lower costs [15].

2. Experimental Set-Up

2.1. PERC Modules

The mono-crystalline 395 W panels with reference JAM54S31/MR/1000V from JA-SOLAR were chosen for studying the PERC technology. These panels present a half-cell configuration, meaning that instead of having one circuit, the panel is divided into two parallel ones, halving the current values. Regarding the Joule loss effect, where the losses are related to the square value of the current, its values drop to one-quarter. There is no reference to using any LID suppression technology for this module, so it was assumed to be nonexistent.

In Figure 6, the electrical parameters at standard test conditions (STCs—irradiance of 1000 W/m^2, cell temperature of 25 °C and an air mass of 1.5) of the PV module are displayed. Note that the module displays 395 W of rated maximum power, corresponding to the values located far to the right in Figure 6.

ELECTRICAL PARAMETERS AT STC

TYPE	JAM54S31 -380/MR/1000V	JAM54S31 -385/MR/1000V	JAM54S31 -390/MR/1000V	JAM54S31 -395/MR/1000V
Rated Maximum Power(Pmax) [W]	380	385	390	395
Open Circuit Voltage(Voc) [V]	36.58	36.71	36.85	36.98
Maximum Power Voltage(Vmp) [V]	30.28	30.46	30.64	30.84
Short Circuit Current(Isc) [A]	13.44	13.52	13.61	13.70
Maximum Power Current(Imp) [A]	12.55	12.64	12.73	12.81
Module Efficiency [%]	19.5	19.7	20.0	20.2
Power Tolerance		0~+5W		
Temperature Coefficient of Isc(α_Isc)		+0.045%°C		
Temperature Coefficient of Voc(β_Voc)		-0.275%/°C		
Temperature Coefficient of Pmax(γ_Pmp)		-0.350%/°C		
STC		Irradiance 1000W/m², cell temperature 25°C, AM1.5G		

Figure 6. Electrical parameters taken from the datasheet of the PERC panel employed in field experiments.

2.2. HJT Modules

The mono-crystalline *MeyerBurger* Glass modules were chosen to study the HJT technology. It presents a half-cell technology, meaning that the Joule loss effect is decreased to one-quarter, and the panel gathers irradiance from both sides due to its natural bi-facial configuration. Figures 7 and 8 display the electrical parameters at the STC of the PV panel. Table 1 is where the most important parameters in STCs are gathered.

Power class in STC² [W_p]				370
Minimum Performance (Power Tolerance −0 W/+5 W) [W_p]				**STC**
Minimum	Power at MPP	P_{mpp}	[W]	370
	Short Circuit Current	I_{sc}	[A]	10.4
	Open Circuit Voltage	V_{oc}	[V]	44.5
	Current at MPP	I_{mpp}	[A]	9.9
	Voltage at MPP	V_{mpp}	[V]	37.7
	Efficiency	η	[%]	20.6

Figure 7. Electrical parameters from the datasheet of the HJT panel N.1 employed in field experiments.

Temperature Coefficients

Temperature Coefficient of I_{SC}	α	[%/°C]	+0.033
Temperature Coefficient of V_{OC}	β	[%/°C]	-0.234
Temperature Coefficient of P_{MPP}	γ	[%/°C]	-0.259
Nominal Module Operating Temperature	NMOT	[°C]	43±3

Figure 8. Electrical parameters from the datasheet of the HJT panel N.2 employed in field experiments.

Table 1. PERC and HJT STC parameters: rated power, efficiency and respective temperature coefficients taken from modules' datasheets.

Module	Max Rated Power [W]	Efficiency [%]	Temp. Coeff. [%/°C]
PERC	395	20.2	−0.350
HJT	370	20.6	−0.259

It is important to note that despite presenting 25 W of the rated power difference, the efficiencies are very similar. Regarding the temperature coefficient, a bigger decrease in the PERC output power is expected with the increase in temperature.

2.3. Location and Connection

The HJT and PERC panels were mounted horizontally side-by-side on the institute's rooftop, as seen in Figure 9.

To connect the panels on the rooftop to the acquisition system, located four floors under, 50 m of PV cables was used and passed through the air conduct, as displayed in Figures 10 and 11.
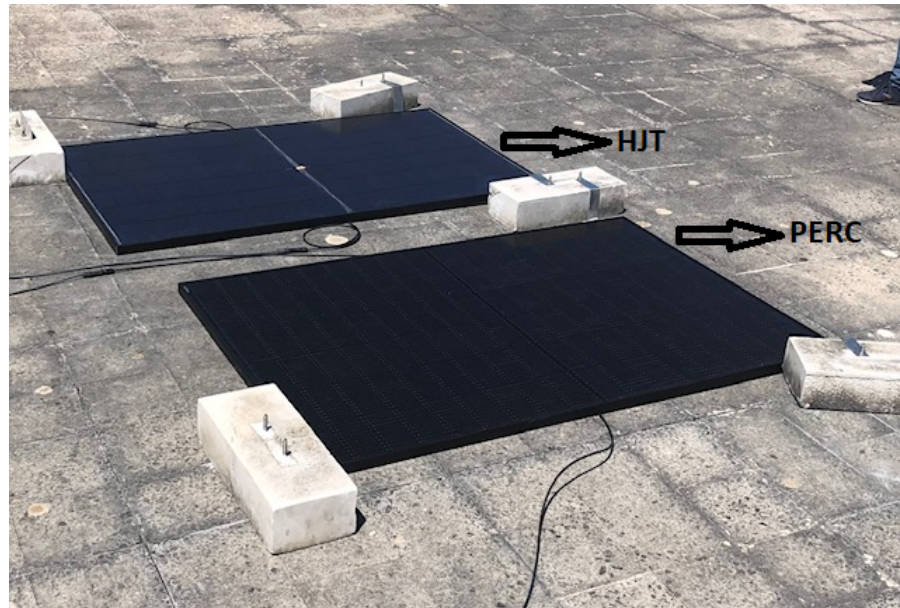
Figure 9. HJT and PERC modules displaced horizontally at the roof.

Figure 10. Expanded roof view of the HJT and PERC modules and their cable connections to our laboratory.

Figure 11. Laboratory photo showing, with a red line, the path of the cables from the roof to the HJT and PERC modules.

2.4. Data Acquisition

The setup displayed in Figure 12 is the acquisition system at the laboratory. The right piece was connected to the HJT module, while the left was connected to the PERC module.

A variable resistor was connected directly to the panel to achieve maximum power, as shown in Figure 12.

This resistor was chosen due to its high current support: 16 A. Also, the resistance range [1 Ω, 9 Ω] is superior to the MPP resistance. For STC conditions, the HJT module displays 37.7 V and 9.9 A at MPP. This way, the correspondent resistance of 3.80 Ω is obtained by Ohm's law $R = \frac{U}{I}$. For the PERC module, MPP is characterized by 30.64 V and 12.61 A, corresponding to 2.41 Ω.

Figure 12. Photo of the system used to analyze the voltage and electric current signals from the HJT and PERC panels. Above the oscilloscope image, the electrical resistance connected to each panel, HJT or PERC, is shown.

A power signal was obtained by visualizing the voltage and current signals, displayed in Figure 13 in yellow and blue, respectively, and multiplying both signals. With the oscilloscope reading the signal during a time interval of 5 s, the resistor values were changed from minimum to maximum. In between, the maximum power point would be visualized by searching for the point of maximum amplitude on the red signal, as seen in Figure 13. Then, visualizing the correspondent current and voltage values on the yellow and blue signals, it was possible to compute the MPP. This approach was taken to collect data on the photovoltaic panels working under load conditions.
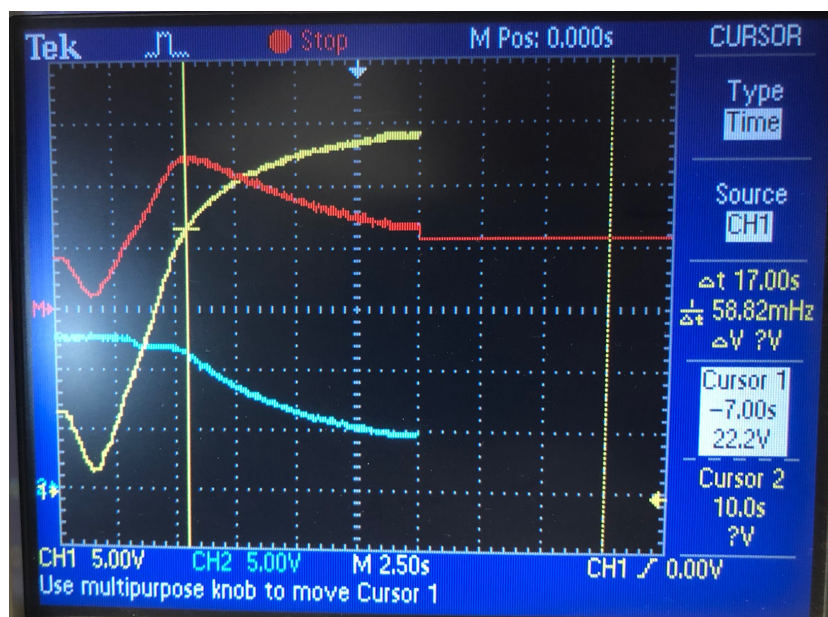

Figure 13. Picture showing the oscilloscope signals of current, voltage and power for one experiment.

3. Results

To evaluate each module's efficiency, Equation (1) was used.

$$\eta = \frac{P_{OUT}}{G \cdot A} \cdot 100[\%] \tag{1}$$

where

- P_{OUT} is the module output power, in W, computed via the oscilloscope;
- G is the horizontal irradiance, in W/m^2;
- A is the module active area. The HJT module area equals 1.793 m^2, and PERC has an area of 1.953 m^2.

Horizontal irradiance measurements were performed with the Pro Solar Power Meter ISM400 shown in Figure 14. Temperature measurements were performed with infrared camera FLIR E6-XT, as shown in Figure 15, always on the same cell on each module.

Data were collected in various weather to obtain a diversified set of samples and evaluate cell technology performance in different conditions. The purpose was to evaluate and compare the differences in performance throughout the day. The experimental results will be shown using two figures displaying the parameters for the desired day: one for module efficiency and temperature and a second for the other for module efficiency, module temperature and now irradiance.

Figure 14. Illustration of the horizontal irradiance acquisition taken on the roof and near the two modules periodically.

Figure 15. Picture of the thermographic camera used to measure and visualize the temperature distribution through the PERC and HJT modules.

3.1. Eighteenth of August—Clear Sky Conditions

All instruments were available to characterize both module performances for the data collection performed on the 18th of August and the remaining days. This way, there are irradiance, module temperature and efficiency values. Throughout the day, no clouds appeared, and both panels received direct radiation from the sun.

Analyzing Table 2 and Figures 16 and 17, it is possible to observe that the HJT panel displayed, on average, 2.37% more efficiency than PERC during this sunny summer day. Except for the value read at 12:15, between 08:30 and 13:00, the irradiance kept increasing. It was expected to visualize an increasing trajectory in efficiency during this time interval, but panel temperature increased as well. It can be seen that the maximum efficiency, 21.91%, was obtained for the HJT panel at 10:15 with a module temperature of 42.1 °C and irradiance of 602 W/m^2. For the PERC panel, however, a maximum efficiency of 17.19% was achieved at 10:45 with a module temperature of 52 °C and irradiance of 677 W/m^2.

How the temperature affects module output is noticeable after both modules present a temperature above the [50 °C; 60 °C] range. Despite the continuous increase in irradiance, efficiency values drop to 11.10% and 9.70% on HJT and PERC, respectively, at 13:00. This behavior reflects the difficulty that solar cells generally present while working under high module temperatures.

Between 12:15 and 14:30, both modules presented temperatures above 64 °C. It would have been expected that even though both panels display very high working temperatures, an increase in irradiance would reflect an increase in efficiency. This was not verified. For high operating temperatures, an increase in irradiance resulted in an efficiency decrease, noticeable in both technologies for the period between 12:15 and 13:00. When irradiance values drop from 1312 W/m^2 at 13:00 to 935.2 W/m^2 at 13:15, a noticeable increase of approximately 4% in each module efficiency was then observed.

When irradiance stabilizes at around 900 W/m^2 and module temperature was between 65 °C and 72 °C, efficiency values fluctuated between 15.53% and 17.81% for HJT and 13.61% and 15.86% for PERC.

The HJT and PERC modules output maximum power at 11:30. The first one displayed 273.80 W, with an efficiency of 19.02% and a module temperature of 64.2 °C. The PERC module displayed 253 W, with an efficiency of 16.14% and a module temperature of 62.2 °C.

Despite module temperature affecting the panel output negatively, the HJT consistently outperformed the PERC panel in terms of efficiency. Looking for module parameters, specifically for the temperature coefficient, it would have been expected that a big difference in power output would appear under the influence of higher temperatures. This was not proved, as the Meyer Burger HJT panel presented a more considerable relative difference (%) regarding PERC in efficiency before the temperatures rose to around 60 °C.

Table 2. Field data collected on August 18th: time, measured HJT output power (Pout-HJT), computed HJT efficiency (Eff-HJT) and measured HJT average temperature (Temp-HJT); measured PERC output power (Pout-PERC), computed PERC efficiency (Eff-PERC), measured PERC average temperature (Temp-PERC) and field measured irradiance.

Time	Pout-HJT	Eff-HJT	Temp-HJT	Pout-PERC	Eff-PERC	Temp-PERC	Irradiance
08:30	56.28	11.05	13.1	60.8	10.96	15	284
08:45	73.00	13.26	16.8	73.65	12.28	17.3	307
09:00	90.79	13.68	22.5	91.13	12.61	21.3	370
09:15	108.56	14.66	26.6	96.48	11.96	23.7	413

Table 2. *Cont.*

| Time	Pout-HJT	Eff-HJT	Temp-HJT	Pout-PERC	Eff-PERC	Temp-PERC	Irradiance
09:30	152.76	16.35	29.9	136.98	13.46	29.1	521
09:45	194.30	19.96	33.4	162.11	15.28	33.4	543
10:00	200.89	18.99	35.3	189.90	16.48	36.1	590
10:15	236.54	21.91	42.1	183.04	15.57	41.2	602
10:30	224.35	18.35	44.6	220.32	16.54	43.6	682
10:45	250.24	20.61	52.9	227.32	17.19	52	677
11:00	258.72	19.66	56.5	222.91	15.55	55.2	733.8
11:15	257.63	18.87	59.5	240.06	16.14	61.8	761.6
11:30	273.80	19.02	64.2	253.08	16.14	62.2	802.8
11:45	256.94	17.10	61.7	234.6	14.33	62.1	838
12:00	245.21	12.85	63.5	239.68	11.53	61	1064
12:15	258.56	16.00	66.2	239.56	13.61	64.8	901.2
12:30	248.86	13	68	241.82	11.6	66.7	1072
12:45	256.22	12.64	69.7	239.4	10.84	68	1130
13:00	261.12	11.10	68.7	248.6	9.70	66.6	1312
13:15	260.38	15.53	68.3	248.64	13.61	65.9	935.2
13:30	262.03	16.47	67.8	250.86	14.47	66.4	887.3
13:45	256.22	17.81	68.6	248.64	15.86	66.3	902.5
14:00	258.56	16.35	71.8	246.24	14.29	68.4	882
14:15	253.79	16.12	70.5	244.2	14.24	70.3	878.3
14:30	257.92	16.19	71	244.08	14.07	69.7	888.5
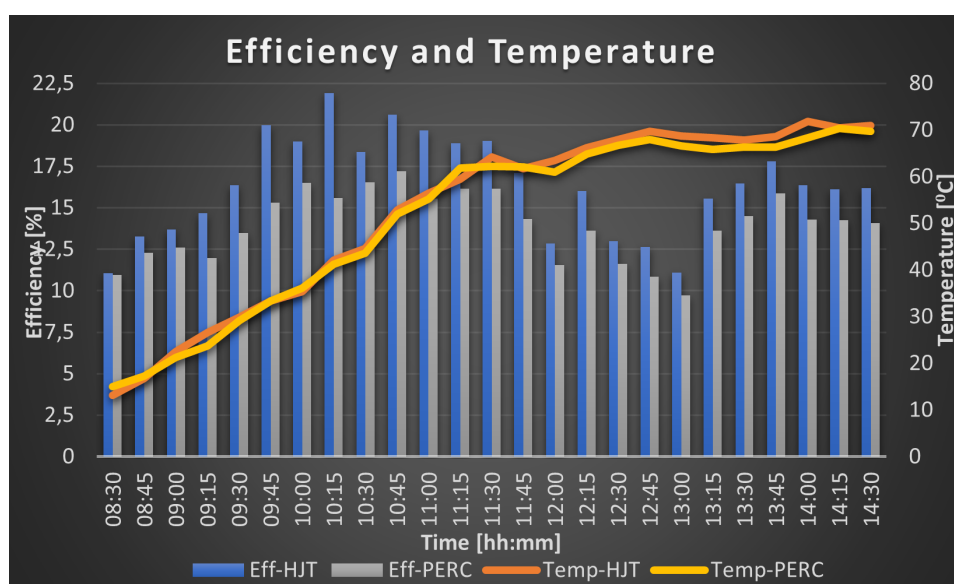
Figure 16. August 18th, between 08:30 a.m. and 02:30 p.m.: evolution of the HJT and PERC efficiencies during this day. Also shown are the average temperatures recorded for each module.
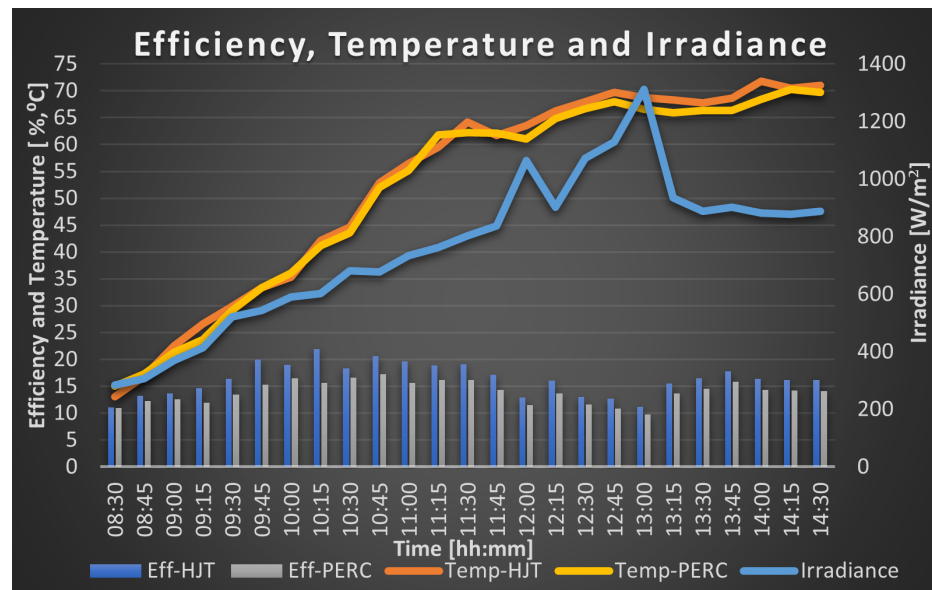
Figure 17. August 18th, between 08:30 a.m. and 02:30 p.m.: evolution of irradiance to show its effects on the modules' temperatures and efficiency.

3.2. Nineteenth of August—Clear Sky Conditions

Parameters that characterize the module's performance were acquired on August 19th. Like the day before, no clouds appeared, meaning that the modules received direct radiation from the sun.

Analyzing Table 3 and Figures 18 and 19, it is possible to observe that the HJT panel displayed, on average, 2.21% more efficiency than PERC during this sunny day.

From 09:15 to 13:15, except for the value read at 12:45, the irradiance slowly rose from 455 to 919.6 W/m^2. It was expected that both panel efficiency would follow this trend. However, the maximum efficiency point registered for HJT appeared at 09:45 with a value of 20.68%, a module temperature of 43.7 °C and an irradiance value of 531.6 W/m^2. At the same time, PERC obtained a maximum daily value of 16.59% efficiency at 10:45 with a module temperature of 55.7 °C and an irradiance value of 719.8 W/m^2.

Module temperature continuously rose in both technologies throughout the day. Figure 18 shows that, at 11:30, the HJT module and PERC module presented 17.75% and 15.64%, respectively. Currently, module temperatures are similar in both technologies, with the HJT presenting 66.2 °C and PERC displaying 65.9 °C. After this time, both modules' temperatures kept rising, surpassing 75 °C, and efficiency values dropped to around 14/15% on HJT and 13% on PERC.

After noon, except for the measurement taken at 12:45, irradiance values were kept inside the [857.7 W/m^2; 919.6 W/m^2] range. Although the module temperature continued to elevate from near 70 °C to near 80 °C, efficiency values were kept nearly constant.

Note that, during the previous day of measurements, on August 18th, between 12:15 and 13:00, while the panels were operating under high temperatures (+60 °C), an increase in irradiance was reflected in a decrease in efficiency. This situation was again verified at 12:45 on August 19th. The HJT panel presented a temperature of 72.6 °C, and the PERC module displayed a temperature of 70 °C. An increase in irradiance from 908.3 to 1185 W/m^2 resulted in a decrease in efficiency of 3.31% for HJT, while PERC dropped 3.01%.

When irradiance dropped from this day's highest value to 917.2 W/m^2, HJT's efficiency value raised 3.44% while PERC saw its efficiency value climb 3.12%. These results indicate that, while performing with high module temperatures, an abrupt increase in irradiance results in a decrease in efficiency, while lowering this significant irradiance value back to the previous values raises efficiency again.

Maximum power was achieved by both modules at 11:30, with the HJT outputting 258.73 W, with a temperature of 66.2 °C and an efficiency of 17.75%. The PERC module outputted 248.4 W, with a temperature of 65.9 °C and efficiency of 15.64%. The irradiance at this time was 813.1 W/m^2.

Performing a similar analysis on the previous day of measurements, the HJT module displayed higher efficiency than the PERC panel during the whole day. Despite outperforming PERC with an average of 2.21% efficiency, this value difference was higher while the modules presented lower temperatures. As the temperature rose from 66 °C, the efficiency difference started to shorten, and, considering the different temperature coefficients, one would have expected to see a higher efficiency difference benefiting the HJT panel in the presence of higher temperatures.

Table 3. Field data collected on August 19th: time, measured HJT output power (Pout-HJT), computed HJT efficiency (Eff-HJT) and measured HJT average temperature (Temp-HJT); measured PERC output power (Pout-PERC), computed PERC efficiency (Eff-PERC), measured PERC average temperature (Temp-PERC) and field measured irradiance.

Time	Pout-HJT	Eff-HJT	Temp-HJT	Pout-PERC	Eff-PERC	Temp-PERC	Irradiance
09:15	118.27	14.50	34.4	99.07	11.15	34.8	455
09:30	145.00	16.10	38.3	140.65	14.33	39.7	502.3
09:45	197.12	20.68	43.7	157.58	15.18	44.4	531.6
10:00	193.76	17.79	45.1	180.14	15.18	45.6	607.5
10:15	228.41	20.53	48.2	185.92	15.34	48.7	620.5
10:30	220.32	17.76	50.2	217.05	16.06	50.8	691.9
10:45	244.35	18.93	55.9	233.23	16.59	55.7	719.8
11:00	253.44	18.64	57.6	236.16	15.95	57.1	758.2
11:15	252.8	17.81	59.7	240.72	15.57	61.8	791.6
11:30	258.73	17.75	66.2	248.4	15.64	65.9	813.1
11:45	245.76	16.46	67.2	232.22	14.28	64.6	832.7
12:00	236.59	15.24	68.3	235.32	13.91	66.8	865.9
12:15	243.04	15.31	70.7	232.96	13.47	68.6	885.2
12:30	237.63	14.59	71	235.4	13.27	69.4	908.3
12:45	239.61	11.28	72.6	237.44	10.26	70	1185
13:00	242.11	14.72	73.6	239.68	13.38	71.2	917.2
13:15	248.68	15.08	75.8	239.4	13.33	73.6	919.6
13:30	243.2	15.49	76.9	237.12	13.86	75.3	875.5
13:45	244.8	15.51	76.6	237.3	13.80	76	880.3
14:00	239.18	14.90	77.1	233.2	13.34	76.2	895.2
14:15	238.33	15.29	78.1	231	13.61	75.3	869
14:30	240.76	15.65	78.1	232.96	13.90	76.7	857.7
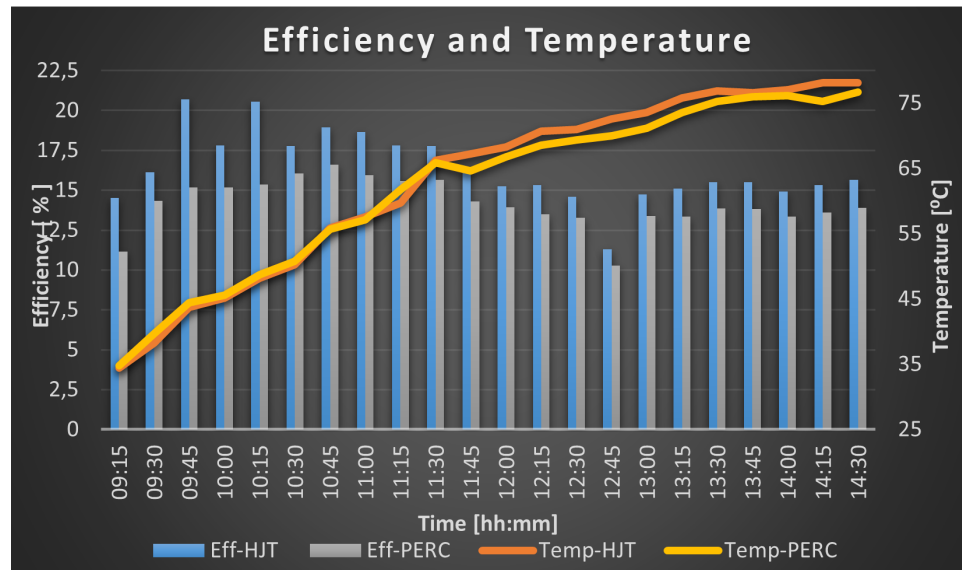
Figure 18. August 19th, between 09:15 and 14:30: evolution of the HJT and PERC efficiencies during this day. Also shown are the average temperatures recorded for each module.
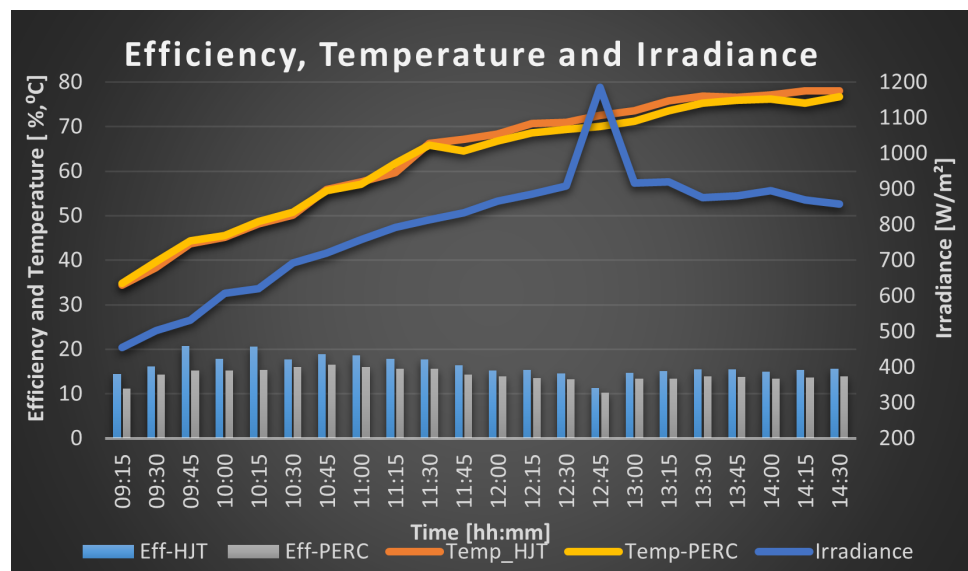
Figure 19. August 19th, between 09:15 and 14:30: evolution of irradiance to show its effects on the modules' temperatures and efficiency.

3.3. Twenty-Fifth of August—Cloudy and Clear Sky Conditions

As can be seen from 09:45 to 12:00 in Table 4 and in Figures 20 and 21, data were collected and low irradiance values were acquired. These reflected the presence of clouds until noon, opening up again and turning into clear sky conditions from 12:15 to 15:30.

Firstly, let us analyze the data acquired in the presence of clouds. For the first time, it can be seen that, in the ten acquisitions performed between 09:45 and 12:00, the PERC module outperformed the HJT module not only once but eight times. During this time, irradiance values were kept below 370 W/m^2, and the modules presented maximum temperatures of 40.6 °C for HJT and 40.9 °C for PERC. On average, the PERC outperformed the HJT module by 3.05% in efficiency during this time. This sounds like a promising value for the PERC technology to work under cloudy conditions. Between 09:45 and 12:00, the PERC module outputted, on average, 86.71 W while the HJT module delivered 69.11 W.

Performing a similar analysis when the sky was free of clouds, from 12:15, it is possible to see that the HJT module outperformed the PERC module until 15:00 regarding module

efficiency. On average, the HJT module was 1.11% more efficient than the PERC module. Looking into the irradiance values during this time was expected to verify this situation, as this parameter never went below 800 W/m^2. Considering the irradiance values, it is possible to divide the analysis into two: one at 12:15 and the other at 13:15. For the first one, it is possible to verify that both modules present better efficiency while the irradiance is below 1000 W/m^2. This was verified while module temperature was between 45 and 46 °C for both technologies.

The analysis performed for the previous days of data concluded that while modules presented high working temperatures, an increase in irradiance would reduce efficiency. This time, the same situation was verified, but the temperature of the modules did not reach 50 °C. It is possible to conclude that a severe increase in irradiance will decrease efficiency independently of the module temperature. This was also verified in the measurements taken at 12:00 and 12:15, where the irradiance values increased from 312.6 W/m^2 to 973.3 W/m^2 and the efficiency dropped from 21.96% to 16.75% on HJT and from 23.58% to 15.02% on PERC. Despite the drop in efficiency values, the power output in HJT went from 123.08 W to 292.4 W, and from 144 W to 285.56 W on PERC.

Starting at 13:15, irradiance values decreased and remained under 900 W/m^2. This resulted in an increase in efficiency regarding the previous measurement, from 12.7% to 16.4% on HJT and from 11.32% to 15.24% on HJT. Despite the significant increase in efficiency, output power decreased slightly in both modules, reducing approximately 14 W and 2 W on HJT and PERC, respectively.

Maximum power was achieved for the HJT module at 12:30 when the module outputted 304.48 W and displayed an efficiency of 17.37%. The temperature displayed was 45.7 °C and irradiance was 977.6 W/m^2. The PERC module achieved maximum power at 12:15 and 12:30, with an output of 285.56 W. Module temperatures were 45 °C and 56 °C, efficiencies were 15.02% and 14.95% and irradiance was 973.3 W/m^2 and 977.6 W/m^2 for the measurements taken at 12:15 and 12:30, respectively.

Table 4. Field data collected on August 29th: time, measured HJT output power (Pout-HJT), computed HJT efficiency (Eff-HJT) and measured HJT average temperature (Temp-HJT); measured PERC output power (Pout-PERC), computed PERC efficiency (Eff-PERC), measured PERC average temperature (Temp-PERC) and field measured irradiance.

Time	Pout-HJT	Eff-HJT	Temp-HJT	Pout-PERC	Eff-PERC	Temp-PERC	Irradiance
09:45	14.68	5.55	24.8	22.17	7.69	24.6	147.6
10:00	35.85	12.80	28.3	58.20	19.08	28.5	156.2
10:15	26.86	13.67	28.3	34.11	15.93	29.3	109.6
10:30	19.84	9.80	26.9	32	14.51	27.6	112.9
10:45	34.52	11.80	28.4	49.10	15.40	28.9	163.2
11:00	67.39	15.08	32.4	112.89	23.19	33.3	249.3
11:15	96.2	16.71	34.6	123.48	19.69	35.4	321.1
11:30	115.2	23.52	36.7	117.6	22.04	37.8	273.2
11:45	157.52	24.015	39.1	173.6	24.296	40.6	365.9
12:00	123.08	21.96	40.6	144	23.58	40.9	312.6
12:15	292.4	16.75	45.1	285.56	15.02	45	973.3
12:30	304.48	17.37	45.7	285.56	14.95	46	977.6

Table 4. *Cont.*

| Time	Pout-HJT	Eff-HJT	Temp-HJT	Pout-PERC	Eff-PERC	Temp-PERC	Irradiance
12:45	264	12.35	51.3	268.4	11.53	51.1	1192
13:00	272	12.70	49.7	264	11.32	48.3	1194
13:15	258.96	16.40	53.4	262.2	15.24	53.5	880.7
13:30	256.88	15.55	55.1	261.96	15.86	54.9	845.7
13:45	257.4	16.67	53	268.8	15.98	51.9	861.3
14:00	260.52	16.79	52.7	264	15.62	52.5	865.5
14:15	257.4	16.63	54	266.2	15.79	51.8	863.3
14:30	258.4	16.85	54.5	261.36	15.64	52.3	855.3
14:45	253.08	17.15	55.3	257.04	15.99	54.1	823.1
15:00	250.12	17.07	55.8	255.2	15.99	55.1	817.3
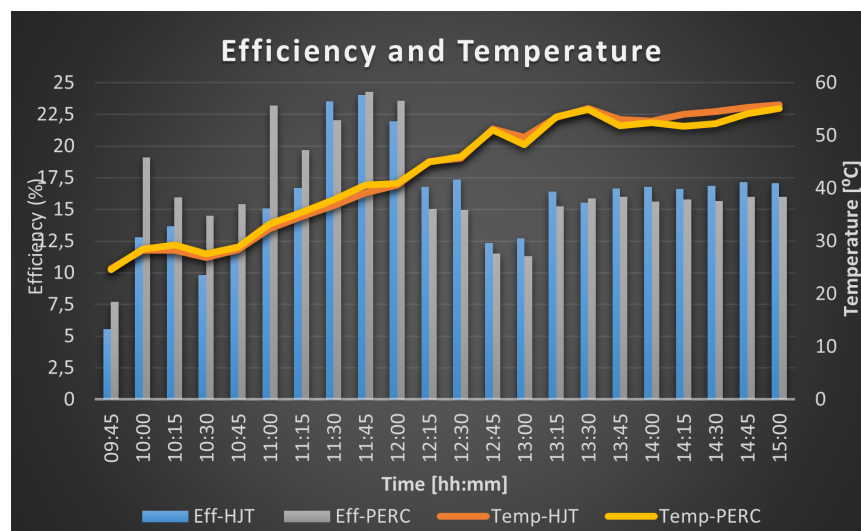
Figure 20. August 29th, between 09:45 and 15:00: evolution of the HJT and PERC efficiencies during this day. Also shown are the average temperatures recorded for each module.
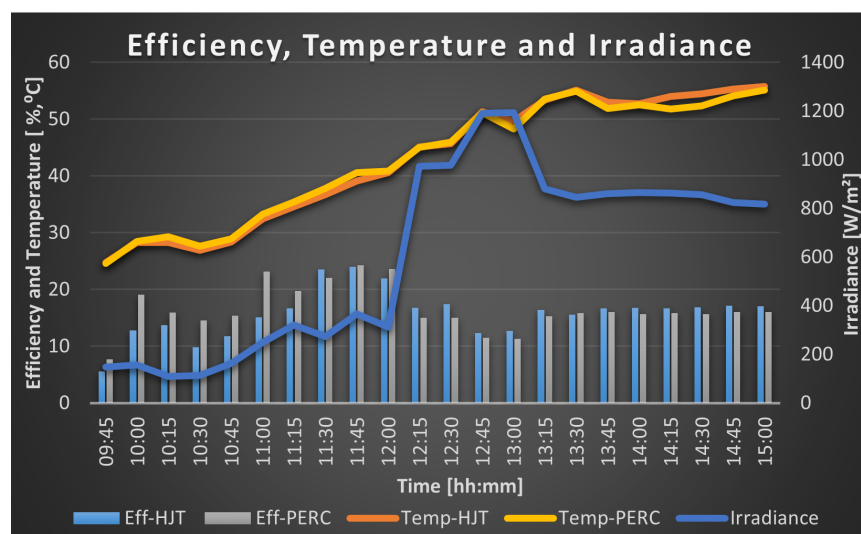

Figure 21. August 29th, between 09:45 and 15:00: evolution of irradiance to show its effects on the modules' temperatures and efficiency.

3.4. Twenty-Ninth of August—Cloudy and Clear Sky Conditions

As can be seen in Table 5, Figures 22 and 23, this day of measurements presented both cloudy, characterized by the low irradiance values from 10:00 to 10:30 and at 11:30, and clear sky situations, characterized by the remaining samples. When performing an analysis when the presence of clouds was confirmed, it is possible to observe that, in the four samples taken, the HJT module outperformed the PERC module in terms of efficiency in three of them. Between 10:00 and 10:30, despite being able to display efficiencies in the [31.71%; 33.80%] range for HJT and [29.43%; 36.59%] range for PERC, the power output of the modules did not exceed 83 W. These high-efficiency values were only verified while the irradiance values were kept below 128 W/m^2. When irradiance values increased to the [700 W/m^2; 900 W/m^2] range, power output increased to the [220 W; 301 W] range, and the HJT modules outperformed the PERC module, regarding efficiency, in all the measurements taken.

Maximum power was achieved by the HJT module at 11:00, displaying an output of 301.93 W. This daily highest value was obtained with an irradiance of 784.3 W/m^2 and a temperature of 55.9 °C, and the module displayed an efficiency of 21.47%. For the PERC module, the maximum outputted power was achieved at 11:15, with a value of 264.46 W, a module temperature of 56 °C, an irradiance value of 821.8 W/m^2 and a module efficiency of 16.48%.

It is possible to observe that, from 10:45 to 15:00, except for the measurements taken at 11:30, the irradiance values were kept above 763 W/m^2. Regarding efficiency, both modules had their values decrease compared to those obtained in the presence of clouds. The PERC module presented efficiency values in the [13.97%; 16.91%] range, while the HJT module displayed values in the [14.96%; 21.47%]. On average, the HJT module displayed 1.47% more efficiency than the PERC module between 10:45 and 15:00, except for the low irradiance measurement at 11:30.

Compared with the previous measurements, the existence of a sudden increase in irradiance was not verified. Instead, at 11:30, a sudden decrease was verified. Irradiance values dropped from 821.8 to 379.9 W/m^2. It is possible to observe that efficiencies on both modules increased, from 17.77 to 20.60% on HJT and from 16.48 to 20.38% on PERC. At the next measurement, irradiance increased to values over 800 W/m^2 again, and, as expected, efficiency values increased.

Table 5. Field data collected on August 29th: time, measured HJT output power (Pout-HJT), computed HJT efficiency (Eff-HJT) and measured HJT average temperature (Temp-HJT); measured PERC output power (Pout-PERC), computed PERC efficiency (Eff-PERC), measured PERC average temperature (Temp-PERC) and field measured irradiance.

Time	Po-HJT	V-HJT	T-HJT	Po-PERC	V-PERC	T-PERC	Irr
09:45	196.5	19.5	/	180.8	16.5	/	561.6
10:00	60.9	33.4	/	58.4	29.4	/	101.6
10:15	77.3	33.8	/	82.9	33.3	/	127.6
10:30	45.8	31.7	/	57.6	36.6	/	80.6
10:45	272.1	19.9	50.1	248.1	16.6	50.4	763.9
11:00	301.9	21.47	55.9	259.08	16.9	52.4	784.3
11:15	261.9	17.8	57.8	264.5	16.5	56	821.8
11:30	140.3	20.6	54.8	151.2	20.4	54.4	379.9
11:45	253.4	17.4	58.2	240.7	15.2	55.4	811.7
12:00	250.4	15.4	59.9	253.1	14.3	58.7	905.7

Table 5. *Cont.*

| Time	Po-HJT	V-HJT	T-HJT	Po-PERC	V-PERC	T-PERC	Irr
12:15	253.8	15.9	61	262.2	15.1	60.2	889.2
12:30	247.00	15.1	61.7	254.4	14.3	60.8	912.7
12:45	286.0	16.2	60.3	277.8	14.4	61.6	985.3
13:00	257.6	15.6	63.3	259.6	14.5	63.1	918.8
13:15	252.8	15.2	69.9	253.1	13.9	69.6	927.7
13:30	249.3	15.8	66	250.9	14.6	64.1	881.7
13:45	257.6	15.9	65.9	252.5	14.3	64.6	902.3
14:00	232.1	15.2	66.3	244.2	14.6	64.9	853.8
14:15	236.2	15.3	66	242	14.4	64.5	861.5
14:30	232.1	15.3	65.7	236.6	14.4	64.3	843.7
14:45	229.8	15.3	63.9	233.2	14.2	63.2	838.3
15:00	220.4	14.9	63.7	232.1	14.5	62.3	821.7
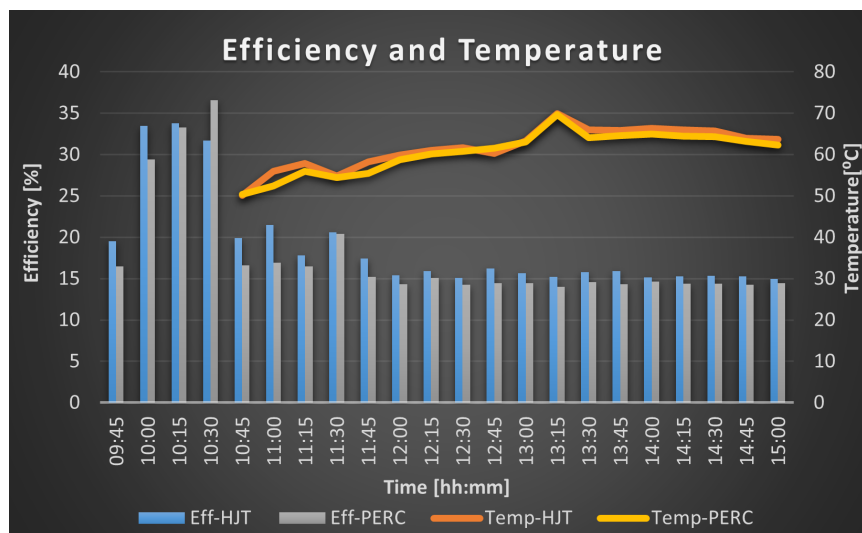
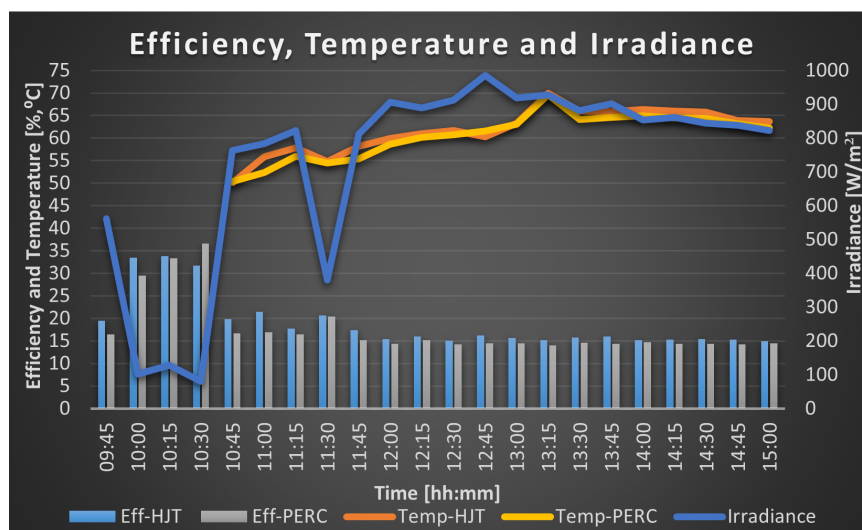**Figure 22.** Module efficiency and module temperature for August 29th.

Figure 23. Irradiance, module efficiency and module temperature for August 29th.

## 4. Temperature and Irradiance Dependencies on HJT and PERC Efficiencies

Temperature coefficients play a crucial role when comparing the performance of PERC and HJT solar modules. The temperature coefficient indicates how much the power output of a solar module decreases as the temperature increases.

PERC modules typically have a temperature coefficient of around -0.33% per °C [14]. They are widely used due to their cost-effectiveness and relatively high efficiency, but they are more affected by high temperatures compared to HJT modules. HJT modules have a lower temperature coefficient of around -0.26% per °C [14]. This lower coefficient means that HJT modules lose less power as the temperature rises, making them more efficient in hot climates due to HJT technology in combining crystalline silicon with amorphous silicon layers, which helps in maintaining higher efficiency even at elevated temperatures.

According to [14], light- and elevated-temperature-induced degradation affects almost every type of silicon wafer, regardless of the doping material, and although the degradation mechanism can recover under normal operation conditions, it is a lengthy process that significantly impacts energy yield and stability. The authors in [14] highlight that hydrogen involvement in the degradation is strongly evidenced, and various hydrogenation methods have been suggested to mitigate this degradation. In [16], temperature coefficients of various silicon solar cell technologies under different illumination conditions were analyzed. The results showed that HJT modules demonstrated superior temperature coefficients under typical field illumination conditions, making them more efficient in real-world scenarios. The research also proposed a method to analyze the temperature coefficient of wide-bandgap chalcogenides, indicating that their values could eventually surpass those of crystalline silicon cells as their open-circuit voltage improves. Both research studies presented in [16] and in [17] also highlighted the importance of considering varying irradiance levels when modeling the performance of PV panels, as temperature coefficients are not constant and can significantly alter with changes in irradiance. At last, and more recently, the study presented in [18] used outdoor measurements collected over up to three years on commercially available solar panels to determine temperature coefficients. This approach provided a more accurate reflection of real-world conditions than standard test conditions. The results confirmed that temperature coefficients are not constant and vary significantly with irradiance. Specifically, the temperature coefficient of voltage increases while the temperature coefficient of power decreases with increasing irradiance. These results underscore the importance of considering real-world conditions in the determination of temperature coefficients for photovoltaic modules to ensure accurate performance predictions.

Considering that previous context, we began several analyses according to each day of meteorological conditions to compute all the efficiency values on the same graph. This way, one can obtain a more detailed analysis of temperature and irradiance behavior. Only the values under clear sky conditions with irradiance over 250 W/m² were selected for this section. This can be justified by the extreme performance difference in the presence of clouds, resulting in very-high-efficiency values translated to minimal power output due to low irradiance.

It is possible to observe in Figure 24 the behavior of HJT and PERC modules' efficiency regarding temperature. As expected, it is possible to note the decrease in efficiency of both modules for temperatures above 55 °C. This statement aligns with the temperature coefficient definition, in which the modules display less efficiency for increased working temperatures. These data display the range [35 °C; 55 °C] of temperature with the best efficiency.
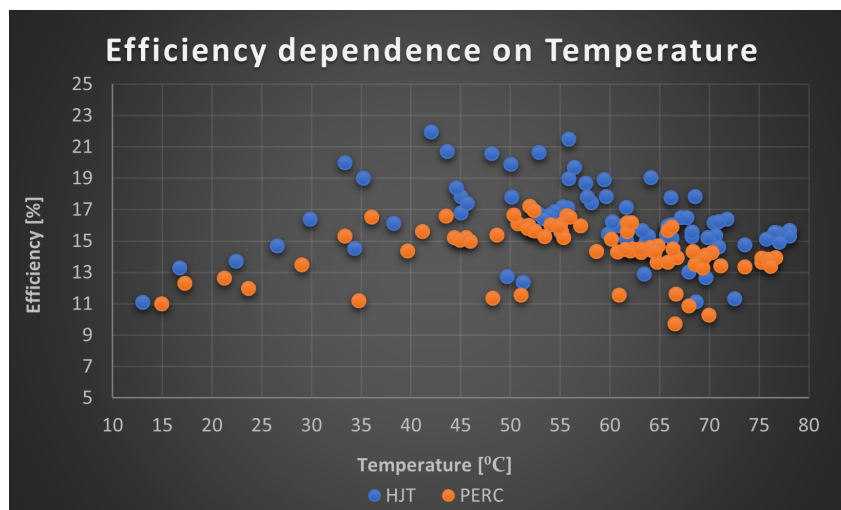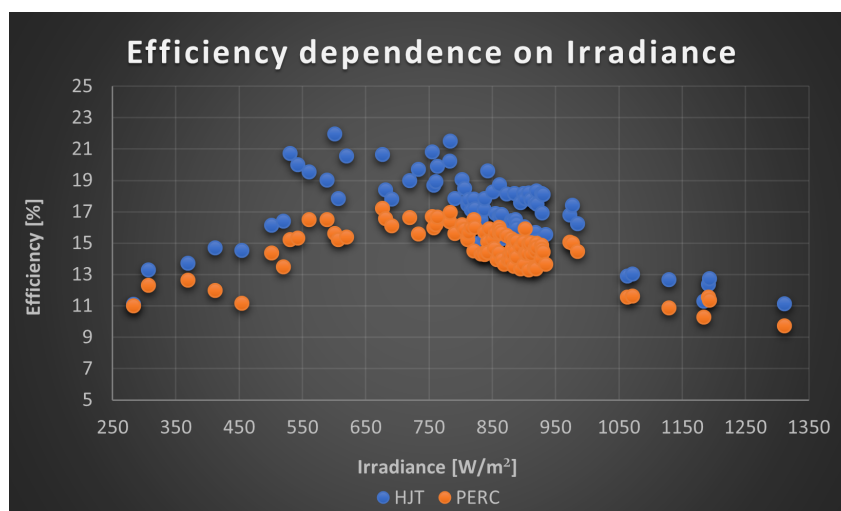
Figure 24. Evolution of how temperature variations impact the performance and efficiency of HJT and PERC solar modules during our field tests.

Figure 25 shows the efficiency dependence of irradiance for the HJT and PERC modules. The data gathered in Figure 25 show an increase in efficiency for both modules until irradiance surpasses 750 W/m^2, approximately. For irradiance values above 1000 W/m^2, efficiency drops to values close to 10% in both modules. A good irradiance range for modules to work is [550 W/m^2; 975 W/m^2]. The individual daily analysis stated that the HJT constantly outperformed the PERC module for clear sky conditions, independently of the irradiance shown.

The effect of temperature on module efficiency was analyzed, but no conclusion was drawn that compared the performance of both modules. It was stated in the analysis of Figure 24 that the effect of temperature resulted in an efficiency decrease. This does not compare the different temperature coefficients presented on the datasheets. The PERC module displays a much higher temperature coefficient of $-0.350\%/^\circ$C compared to the $-0.259\%/^\circ$C parameter of the HJT.

In Figure 26, the temperature dependence of the modules' efficiency difference is shown. According to the temperature coefficient values, a bigger difference in efficiency was expected to be seen that would favor the HJT module when entering high temperatures. This was not verified, as the modules present higher differences on temperatures below 50 $^\circ$C.

Figure 25. Evolution of how irradiance magnitude impacts the efficiency of HJT and PERC solar modules.
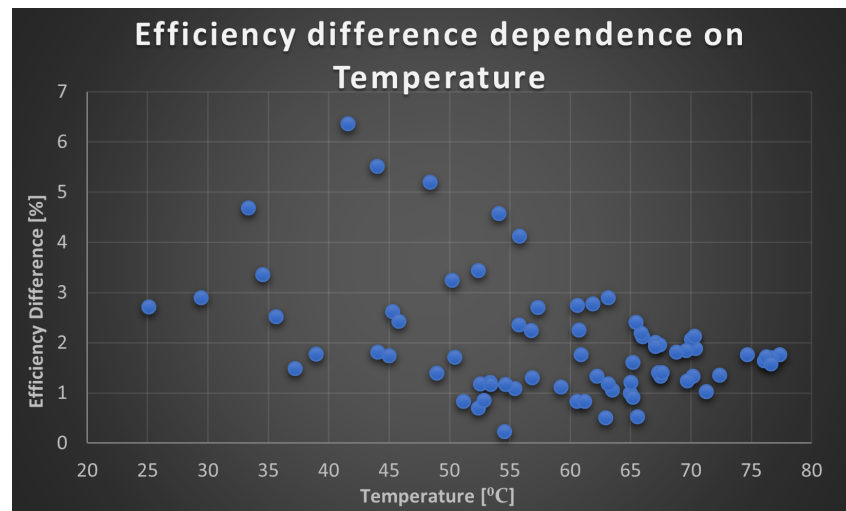
Figure 26. Evolution of how temperature impacts the efficiency of HJT and PERC solar modules.

5. Discussion

After analyzing five days of collected data, the most important information is gathered below:

- Under clear sky conditions, regarding efficiency, the HJT constantly outperforms the PERC module;
- Under cloudy conditions, regarding efficiency, the PERC module displayed higher values than the HJT module in 71.4% of the measurements;
- Despite the PERC module presenting higher power output in STC conditions, experimentally, the HJT module outputs, almost every time, more power than the PERC module;
- A sudden increase in irradiance negatively affects the efficiency, independently of the module temperature as shown in Figure 27. Likewise, a sudden decrease in irradiance will increase module efficiency;
- For the HJT module, maximum power was obtained with an average irradiance of 859.62 W/m^2, an average efficiency of 18.78% and an average temperature of 58 °C;
- For the PERC module, maximum power was obtained with an average irradiance of 866.26 W/m^2, an average efficiency of 15.65% and an average temperature of 60.03 °C;
- Despite the HJT module displaying a better temperature coefficient, the efficiency difference is shortened when the modules present high working temperatures;
- Modules display better efficiency when working under the irradiance range [550 W/m^2; 975 W/m^2];
- Modules display better efficiency when working under the temperature range [35 °C; 55 °C].

Our results show the impact of sudden changes in irradiance on the PERC and HJT modules in terms of their energy output. The underlying physics of these irradiance changes involve atmospheric conditions, geographical location and temporal factors, which influence the amount of solar radiation reaching the PV modules. Mitigation strategies typically include energy storage systems to buffer energy supply, advanced forecasting to predict and manage changes and power electronic technologies to balance load and maintain stability.

The research in [19] aimed to improve the efficiency of photovoltaic systems (PVSs) when used in electric vehicles (EVs), aiming to mitigate sudden irradiance changes by proposing a sensorless MPPT technique that does not rely on irradiance sensors. The proposed technique, DS-ANN, is based on the manufacturer datasheet parameters as

inputs to an artificial neural network (ANN). The training was performed using Bayesian backpropagation–regularization, ensuring that the technique works across different PV modules without retraining. The DS-ANN technique was validated using simulations with 20 commercial PV modules against actual irradiance data. The results indicated a robust and efficient solution for MPPT in EVs, especially under varying irradiance conditions caused by shadows from clouds, buildings, and other structures.
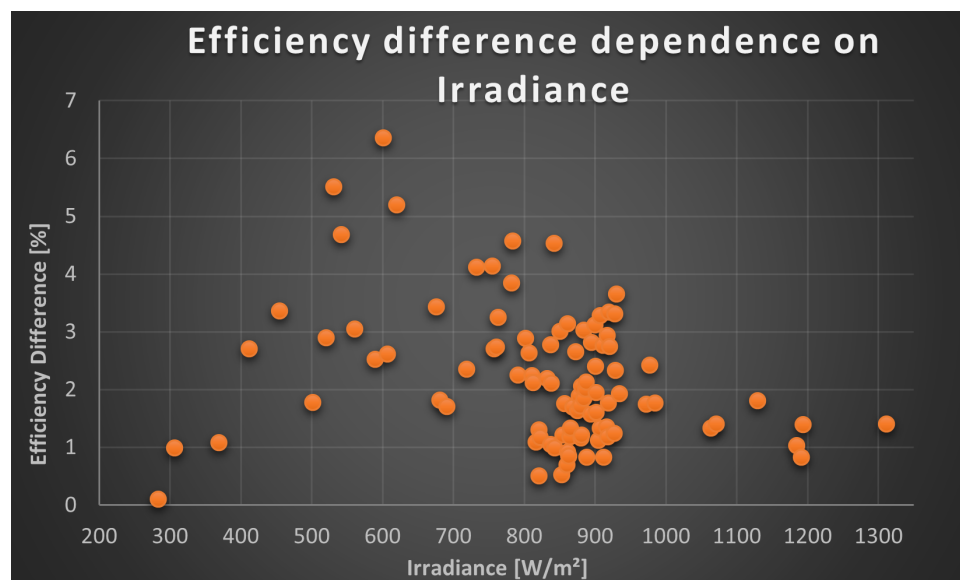
Figure 27. Investigating how variations in irradiance levels affect the efficiency differences between HJT and PERC modules.

Another approach without any machine learning method was presented in [20]. It investigated four types of incremental conductance (INC) methods: fixed step size (FSIC), variable step size (VSIC), first proposition of a modified variable step size (MVS1IC), and second proposition of a modified variable step size (MVS2IC). The results indicated that the MVS2IC method outperforms the other ones in terms of tracking speed and accuracy, making it the most efficient for charging battery loads from PV modules. This research highlights the importance of selecting appropriate step sizes in INC methods to optimize the performance of MPPT in varying environmental conditions.

A different research study was shown in [21]. The authors tested the feasibility of using all-sky imagers (ASIs) to forecast solar irradiance ramp events, which are sudden changes in solar irradiance due to cloud movements. Their research concluded that ASI-based nowcasts are valuable for predicting solar irradiance ramp events, and they also suggested combining physical and deep-learning-based methods to improve forecast accuracy.

All of our results also highlight how the efficiencies of both the PERC and HJT modules are affected by temperature. Predictive modeling was recently applied in [22], generalizing its findings beyond the specific weather scenarios tested. The effectiveness of artificial neural networks (ANNs) and multiple linear regression (MLR) was compared to predict the efficiency of photovoltaic systems under varying weather conditions. Even with limited data availability, the authors showed that ANNs outperform MLR in capturing the complex relationships between environmental factors and photovoltaic efficiency. Instead, the research in [23] used a long-term memory recurrent neural network (LSTM-RNN) model. Two forecasting strategies, one recursive and the other a non-recursive multiple-input and multiple-output (MIMO), were tested using five years of data from a PV power plant in Cluj-Napoca, Romania. From the predictive ANN models, the LSTM-RNN model was one with high prediction accuracy, with performance metrics such as root mean square error,

mean bias error and mean average error, indicating its effectiveness in predicting electric power production. More recently, ANNs have been used to predict solar irradiance in urban areas [24]. The urban attributes of 20 cities were used to train the ANN model, which predicted solar irradiance with high precision. Their findings emphasize the importance of integrating solar irradiance predictions into urban planning to optimize solar energy use and support sustainable city development.

Previous research underscores the need for more comprehensive models to accurately predict efficiency across various conditions. For example, some materials may exhibit higher efficiency at lower irradiance as a result of their bandgap properties, while others perform better under high-irradiance conditions. The review published in [25] indicates that solar absorbance, electrical efficiency, transmittance of the PV module glass cover, irradiance, ambient temperature and wind speed are key parameters to consider. Their review analyzed 33 correlations for estimating the operating temperature of PV cells, highlighting those key parameters set. The results provide information on best practices for obtaining accurate temperature measurements and emphasize the need for reliable models to predict PV model performance under varying weather conditions.

Case Study and Economical Analysis

After analyzing the experimental data, it is possible to compute the average efficiencies of the modules necessary to perform economical analysis and to make conclusions about project feasibility and break-even points.

The modules' performance under cloudy conditions was not considered for this calculation since they represent much higher efficiency values with low power output. This way, the following averages, according to each measurement day, were computed and displayed in Table 6.

Note that these values represent the efficiency of the system (modules+cable). Using the software PVGIS [26], the monthly irradiation, in [kWh/m^2], over one year, was computed and is displayed in Figure 28. These values were computed considering the horizontal mounting of the modules on the university location. To compute the module energy output, Equation (2) was used, and the values obtained are displayed in Table 7 and in Figure 29.

Table 6. Daily and average efficiencies of the HJT and PERC modules: August 2nd, 18th, 19th and 29th.

Day	HJT Efficiency [%]	PERC Efficiency [%]
August 2nd	18.31	15.20
August 18th	16.31	13.94
August 19th	16.37	14.16
August 25th	16.02	14.91
August 29th	16.52	14.96
Average	16.51	14.63

$$\text{Energy Output} = \text{Total Irradiance} \cdot \text{Module Total Area} \cdot \eta \qquad (2)$$

Searching for different electricity suppliers in Portugal for 2022 and their respective tariffs, Table 8 was computed. As several values are displayed, and there is a substantial difference between the least and the most expensive tariff, the average value of 0.18424 EUR/kWh was considered to result in a fair analysis.
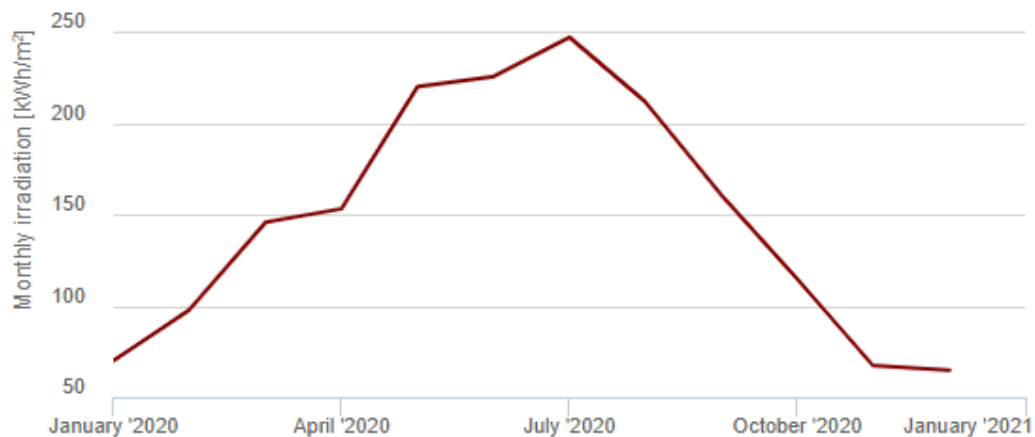
Figure 28. Monthly irradiation during the year 2020.

Table 7. Total energy conversion estimated for HJT and PERC modules during one year.

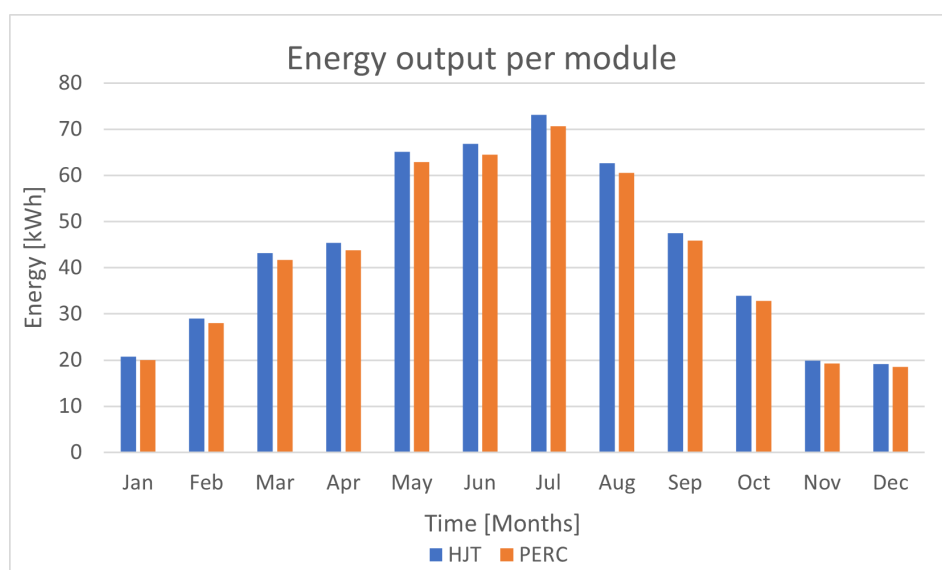| Month	Total Irradiance [kWh/m^2]	HJT Output [kWh]	PERC Output [kWh]
January	69.96	20.71	19.98
February	97.97	29.00	27.99
March	145.81	43.15	41.66
April	153.19	45.34	43.76
May	220.1	65.14	62.88
June	225.65	66.78	64.47
July	247.2	73.16	70.62
August	211.85	62.70	60.52
September	160.63	47.54	45.89
October	114.76	33.96	32.79
November	67.25	19.90	19.21
December	64.78	19.17	18.51
Total	1779.15	526.56	508.28

Figure 29. Energy output per month of one HJT module and one PERC module.

Table 8. Electric energy suppliers operating in Portugal and their tariffs during 2022.

Suppliers	kWh [EUR]
EDP commercial	0.2377
Goldenergy	0.1465
Endesa	0.1449
Iberdrola	0.1491
Galp Energia	0.243

The values in Table 7 consider the system used in the laboratory experiments. However, five projects will be computed to analyze the economic feasibility of using these different modules. The first three projects will cover fixed power installations. These simulate a situation where the system's constraint is total power installed. Since both modules present similar nominal power per square meter, 206.40 W/m^2 on HJT and 202.28 W/m^2 on PERC, the power constraint is equivalent to having an area constraint. Results from these cases will conclude which technology is best suited to be implemented on installations like house rooftops, factories' rooftops and photovoltaic parks.

Two other projects with fixed investment costs will be simulated. The installation constraint is now the system's cost. Results from these cases will conclude which technology is better suited to be implemented in situations where the system area is now not considered.

6. Projects with a Fixed Power Installation

6.1. 4.5 kW Project

An installation of 4.5 kW was considered. This case compares 12 PERC modules, with 4740 W in STC, and 13 HJT modules, referenced with 4810 W in STC. This way, the η for each of (module + cables) is the same value verified in Table 6: 16.51% for HJT and 14.63% for PERC.

It is mandatory to compute the average power output to choose an inverter that displays higher efficiency with the system power output. Considering that a day has, on average, 8 h of sun throughout the year, as well as the data presented in Table 7, module power was achieved by dividing the monthly energy output by the total hours of daylight during a month, presented in Table 9 and in Figure 30.

Table 9. Average power estimated to be delivered by each HJT and PERC module for each month.

Month	Power HJT [W]	Power PERC [W]
January	83.49	80.59
February	129.44	124.95
March	174.01	167.97
April	188.90	182.35
May	262.66	253.54
June	278.26	268.60
July	295.00	284.76
August	252.81	244.04
September	198.08	191.20
October	136.95	132.19
November	82.93	80.05
December	77.30	74.62

The month with the highest average power production is July, with an average of 295 W delivered on HJT and 284.76 W outputted on PERC. Knowing that the system is composed of 13 HJT modules and 12 PERC modules, the system will output, on average, in July, 3835 W for the HJT system and 3417.12 W for the PERC system. Based on these values and consulting the market, choosing the best inverters for each system is possible. For the HJT system, the PRIMO 4.0-1 with 4000 W nominal power was chosen. The PRIMO 3.5-1 inverter with 3500 W nominal power was then chosen for the PERC system. Both are manufactured by Fronius International GmbH, which is based in Wels, Austria.
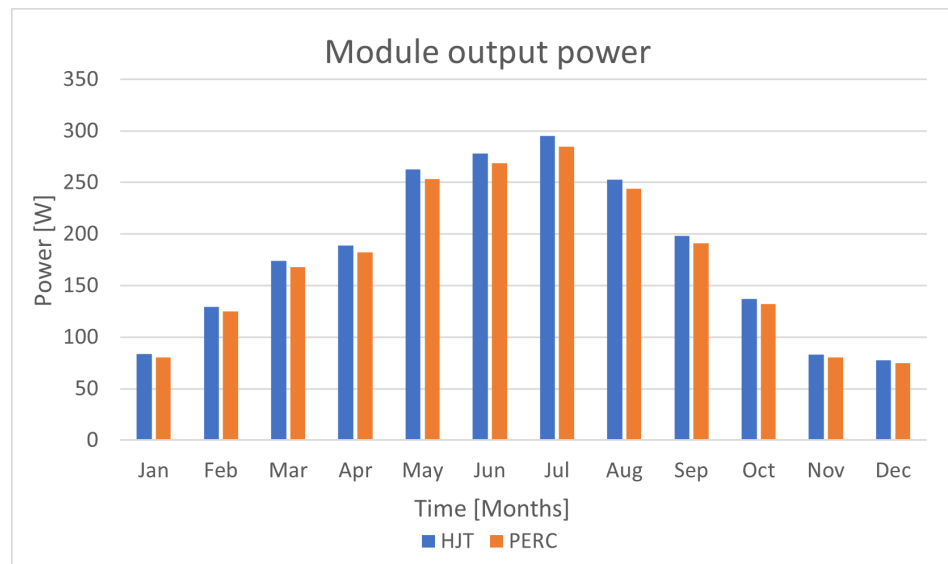
Figure 30. Average power delivered by the HJT and the PERC module for each month.

Inverter efficiencies strongly depend on the available power input. This results in a variation in the inverter efficiency during the year that must be considered when calculating this project. As stated in Table 9, 295 W was the average power produced in July for HJT, while 284.76 W corresponded to the PERC module. Table 10 displays the annual system average output divided by the nominal power of the inverter.

Table 10. Average monthly system power divided by inverter nominal power.

Month	Power HJT [%]	Power PERC [%]
January	27.13	27.63
February	42.07	42.84
March	56.55	57.59
April	61.40	62.52
May	85.37	86.93
June	90.44	92.09
July	95.88	97.63
August	82.17	83.67
September	64.38	65.56
October	44.51	45.33
November	26.95	27.45
December	25.12	25.59

Figure 31 displays the inverter efficiency regarding the input power. It is possible to observe in Figure 31 that there are three displayed efficiencies for each nominal power value. This is verified due to the different behaviors that the inverter displays when different voltage levels are available on the input. As this project case is based on power input/output, an average of these three voltages was performed and is displayed in Table 11. With Table 10, it is possible to display the inverter efficiency for each month of the year, as shown in Table 12.

EFFICIENCY	PRIMO 3.5-1	PRIMO 4.0-1
Max. efficiency	98.0 %	98.0 %
European efficiency (η_{EU})	96.8 %	97.0 %
η at 5 % $P_{ac,r}$ [2]	80.8 / 82.5 / 82.5 %	80.8 / 82.5 / 82.5 %
η at 10 % $P_{ac,r}$ [2]	86.3 / 93.6 / 91.8 %	86.6 / 93.9 / 92.2 %
η at 20 % $P_{ac,r}$ [2]	91.6 / 96.2 / 95.2 %	92.2 / 96.7 / 95.6 %
η at 25 % $P_{ac,r}$ [2]	92.7 / 96.9 / 95.8 %	93.2 / 97.2 / 96.1 %
η at 30 % $P_{ac,r}$ [2]	93.5 / 97.2 / 96.3 %	94.0 / 97.2 / 96.8 %
η at 50 % $P_{ac,r}$ [2]	95.0 / 97.7 / 97.3 %	95.2 / 97.8 / 97.4 %
η at 75 % $P_{ac,r}$ [2]	95.6 / 97.8 / 97.8 %	95.8 / 97.9 / 97.8 %
η bei 100 % $P_{ac,r}$ [2]	95.8 / 98.0 / 97.8 %	95.9 / 98.0 / 97.9 %

Figure 31. Showing how inverter efficiency changes with respect to the power input. Case for a fixed power installation of 4.5 kW.

Table 11. Inverters efficiencies related to primary power and module technology.

| Efficiency	Efficiency for HJT [%]	Efficiency for PERC [%]
η at 25% of $P_{ac,r}$	95.50	95.13
η at 30% of $P_{ac,r}$	96.00	95.67
η at 50% of $P_{ac,r}$	96.80	96.67
η at 75% of $P_{ac,r}$	97.17	97.07

Table 12. Monthly estimated inverter efficiencies.

Month	HJT Inverter Efficiency [%]	PERC Inverter Efficiency [%]
January	95.50	95.13
February	96.00	95.67
March	96.80	96.67
April	96.80	96.67
May	97.17	97.07
June	97.17	97.07
July	97.17	97.07
August	97.17	97.07
September	96.80	96.67
October	96.00	95.67
November	95.50	95.13
December	95.50	95.13

It is now possible to compute and compare the final energy output of each system. Applying the inverter efficiencies present in Table 12 to the module's energy output present

in Table 7 and multiplying by the number of modules in each system, it is possible to obtain the final energy outputted by each system monthly and annually, as can be seen in Table 13 and in Figure 32.

Table 13. Monthly and yearly estimated energy produced by 13 HJT and 12 PERC modules.

| Month	Energy Produced HJT [kWh]	Energy Produced PERC [kWh]
January	257.06	228.17
February	361.86	321.31
March	543.05	483.21
April	570.53	507.67
May	822.83	732.42
June	843.58	750.89
July	924.14	822.60
August	791.99	704.97
September	598.24	532.32
October	423.87	376.38
November	247.10	219.33
December	238.02	211.27
Annual	**6622.28**	**5890.55**
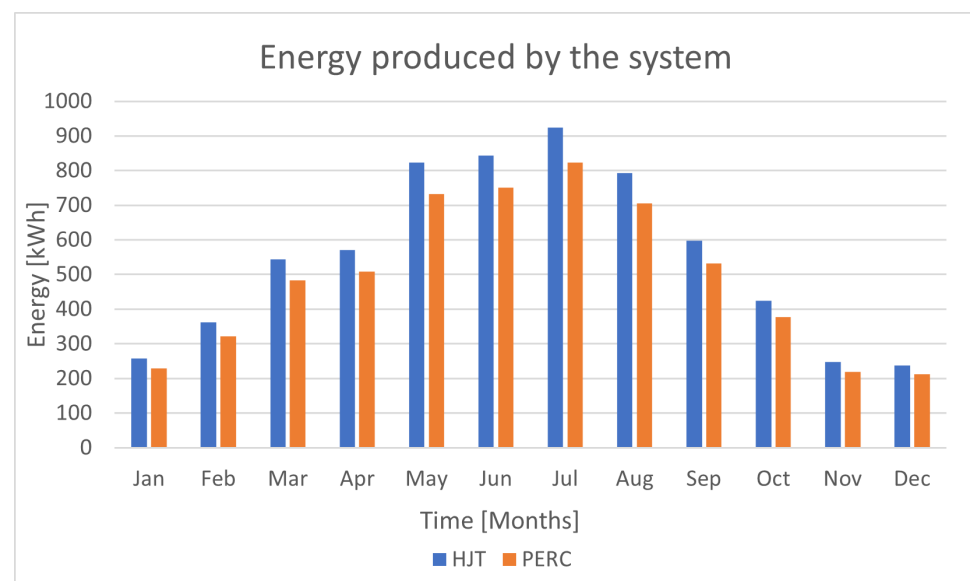
Figure 32. Energy produced by HJT and PERC system for a year. Case for a fixed power installation of 4.5 kW.

With an annual production of 6622.28 kWh for the HJT system and 5890.55 kWh for the PERC system and considering an average price of 0.18424 EUR/kWh, it is possible to save annually EUR 1220.09 and EUR 1085.27 with the HJT and PERC system, respectively. There is a maximum degradation of 0.20 % of nominal power per year for the HJT module, and the manufacturer displays both power and product warranty for 30 years. For the PERC module, the manufacturer displays a degradation of 0,55% of nominal power per year while offering a 12-year product and 25-year linear power output warranty. It is then possible to compute the monetary value of the converted energy accounting for degradation

during 30 years, as seen in Table 14 and in Figure 33. It is also possible to compute the cumulative production for 12, 15, 20 and 30 years as displayed in Table 15.

Table 14. Estimated annual revenue of HJT and PERC system accounting for module degradation for 30 years.

Year	HJT [EUR]	PERC [EUR]	Year	HJT [EUR]	PERC [EUR]	Year	HJT [EUR]	PERC [EUR]
1	1217.65	1079.33	11	1193.57	1021.73	21	1162.98	967.20
2	1215.22	1073.43	12	1191.18	1016.14	22	1160.66	961.90
3	1212.80	1067.56	13	1188.81	1010.58	23	1158.34	956.64
4	1210.38	1061.72	14	1186.43	1005.05	24	1156.03	951.41
5	1207.96	1055.91	15	1184.07	999.55	25	1153.72	946.21
6	1205.55	1050.14	16	1181.70	994.09	26	1151.42	941.03
7	1203.14	1044.39	17	1175.82	988.65	27	1149.12	935.88
8	1200.74	1038.68	18	1173.48	983.24	28	1146.83	930.76
9	1198.35	1033.00	19	1167.64	977.86	29	1144.54	925.67
10	1195.95	1027.35	20	1165.31	972.51	30	1142.26	920.61
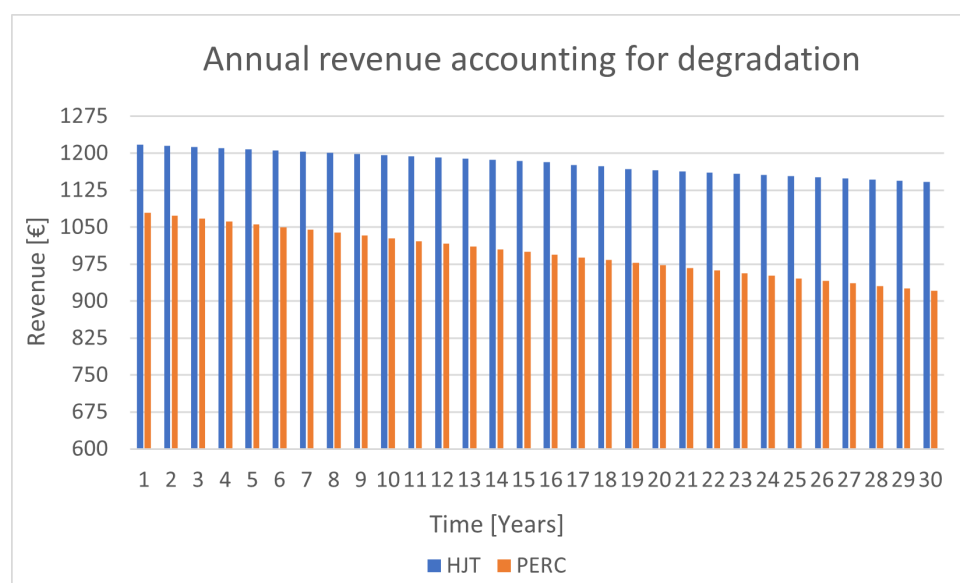
Figure 33. Annual revenue of HJT and PERC system accounting for module degradation for 30 years. Case for a fixed power installation of 4.5 kW.

Table 15. Cumulative revenues of systems using both technologies for 12, 15, 20 and 30 years.

Time [years]	Revenues HJT [EUR]	Revenues PERC [EUR]	Revenue Difference [EUR]
12 years	14,452.50	12,569.36	1883.14
15 years	18,011.81	15,584.55	2427.26
20 years	23,875.76	20,500.91	3374.85
30 years	35,401.68	29,938.23	5463.45

After computing the production of the systems using HJT and PERC technology, it is now required to compute the respective costs. The HJT module was sold for EUR 271.385 per unit when this research was performed. Hence, EUR 3528 was the value to pay for

13 modules. Regarding PERC technology, modules had a unitary price of EUR 154.16. Twelve modules would cost EUR 1849.92.

Regarding inverters, the PRIMO 4.0-1 had a cost of EUR 1389.00 [27] for the HJT system, while the PRIMO 3.5-1 had a cost of EUR 1314.99 [28] for the PERC system.

Regarding cables, 100 m was sold for EUR 140. With an approximate usage of 200 m of cables for each system, EUR 280 was added to the cost of each system. A horizontal structure that supports more than 10 modules was considered to assemble both systems on horizontal rooftops and cost EUR 781.82. Finally, EUR 1000 was considered as the cost of labor for assembling the whole system.

Considering all previous costs, the final system prices can be displayed in Table 16.

With the costs and the production of the systems computed, it is possible to see in Figure 34 the cumulative profits of these systems for 30 years. In Table 17, it is possible to observe the profits for years 12, 15, 20 and 30, as well as the average profit per year (APpY) and the average return on investment (AROI) by year. The APpY value can be computed by dividing the cumulative profit for a selected year by the number of years since the investment has begun, displayed in Equation (3). AROI can be calculated as displayed in Equation (4). Note that this equation is similar to the return on investment (ROI) Equation (5), but instead of considering the annual profit, it considers the cumulative profit until the designated year.

Table 16. HJT and PERC estimated system costs for 4.5 kW system.

Material	HJT [EUR]	PERC [EUR]
Modules	3528.01	1849.92
Inverters	1389.00	1314.99
Cables	280	280
Structure	781.82	781.82
Labor	1000	1000
Total	6978.83	5226.73
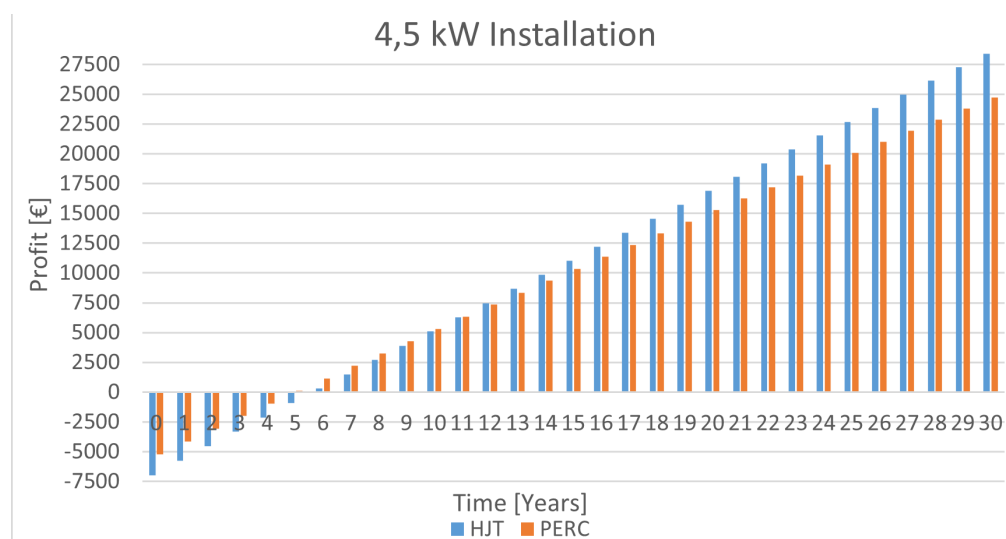
Figure 34. Cumulative profits of HJT and PERC systems throughout 30 years—4.5 kW fixed power installation.

$$APpY = \frac{CumulativeProfit}{Year} \tag{3}$$

$$AROI = \frac{Cumulative Revenues - Costs}{Costs} = \frac{Cumulative Profit}{Costs} \qquad (4)$$

$$ROI = \frac{Revenues - Costs}{Costs} \qquad (5)$$

Table 17. Cumulative, APpY and AROI for 10, 12, 15, 20 and 30 years—4.5 kW installation.

Years	HJT Revenue [EUR]	PERC Revenue [EUR]	APpY HJT [EUR]	APpY PERC [EUR]	AROI HJT [%]	AROI PERC [%]
10	5088.97	5304.77	508.90	530.48	7.29	10.15
12	7473.68	7342.64	622.81	611.89	8.92	11.7
15	11,032.99	10,357.82	735.53	690.52	10.54	13.21
20	16,896.94	15,274.18	844.85	763.71	12.1	14.61
30	28,422.85	24,711.51	947.43	823.72	13.58	15.76

The results obtained indicate that the PERC system would achieve the break-even point, where costs and revenues cancel each other, during the 5th year, while the HJT system would achieve the break-even point during the 6th year. After this time, they will turn into a lucrative investment. It is possible to see in Figure 34 that, despite displaying more costs and therefore lowering the annual return on investment, the HJT system can be considered a better investment and will deliver more profit over the long run. During the 12th year, the HJT system surpasses the revenue of the PERC system and displays a better average profit per pear over long periods.

6.2. A 3.5 kW Project

To simulate a 3.5 kW project, ten modules were considered for the HJT system and nine for the PERC system. The remaining costs, such as cables, horizontal structure, inverters and labor, were assumed to be the same as in the previous case. System costs are visualized in Table 18. With the costs and the production of the systems computed, it is possible to see in Figure 35 the cumulative profits of these systems for 30 years. In Table 19, it is possible to observe the profits for years 12, 15, 20 and 30, as well as the APpY and AROI.

Table 18. HJT and PERC system costs for 3.5 kW system.

Material	HJT [EUR]	PERC [EUR]
Modules	2713.85	1387.44
Inverters	1389.00	1314.99
Cables	280	280
Structure	781.82	781.82
Labor	1000	1000
Total	6164.67	4764.25

For a 3.5 kW case, the PERC system would achieve the break-even point during the 6th year, while the HJT system would achieve the break-even point during the 7th year. After this time, they will turn into a lucrative investment. Similar to the 4.5 kW installation, in the long run, the HJT system will deliver more profits than the PERC system despite the bigger investment costs and having a lower annual return on investment. During the 11th year, the HJT system will surpass the revenue of the PERC system.
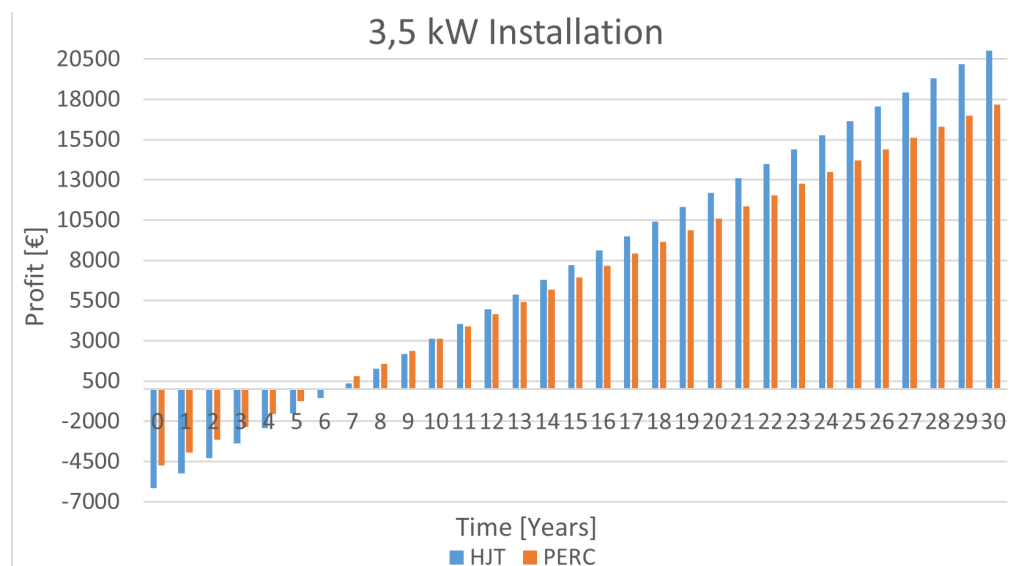
Figure 35. Cumulative profits of HJT and PERC systems throughout 30 years—3.5 kW fixed power installation.

Table 19. Cumulative, APpY and AROI for 10, 12, 15, 20 and 30 years—3.5 kW installation.

Years	HJT Revenue [EUR]	PERC Revenue [EUR]	APpY HJT [EUR]	APpY PERC [EUR]	AROI HJT [%]	AROI PERC [%]
10	3118.22	3134.38	311.82	313.44	5.06	6.58
12	4952.64	4662.78	412.72	388.56	6.70	8.16
15	7690.57	6924.17	512.71	461.61	8.32	9.69
20	12,201.31	10,611.43	610.07	530.57	9.90	11.14
30	21,067.39	17,689.43	702.25	589.65	11.39	12.38

6.3. A 2.5 kW Project

To simulate a 2.5 kW project, seven modules were used for the HJT and PERC systems. The remaining costs, such as cables, horizontal structure, inverters and labor, were assumed to be the same. System costs are visualized in Table 20. With the costs and the production of the systems computed, it is possible to see in Figure 36 the cumulative profits of these systems for 30 years. In Table 21, it is possible to observe the profits for years 12, 15, 20 and 30, as well as the APpY and AROI.

Table 20. HJT and PERC system costs for 2.5 kW system.

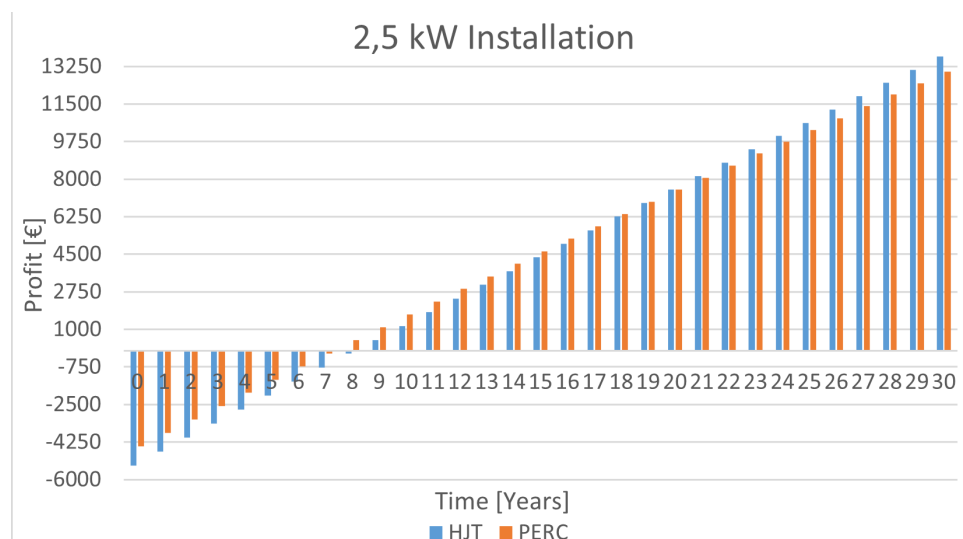| Material	HJT [EUR]	PERC [EUR]
Modules	1899.70	1079.12
Inverters	1389.00	1314.99
Cables	280	280
Structure	781.82	781.82
Labor	1000	1000
Total	5350.52	4455.93

Figure 36. Cumulative profits of HJT and PERC systems for 30 years—2.5 kW fixed power installation.

Table 21. Cumulative, APpY and AROI for 10, 12, 15, 20 and 30 years—2.5 kW installation.

Years	HJT Profit [EUR]	PERC Profit [EUR]	APpY HJT [EUR]	APpY PERC [EUR]	AROI HJT [%]	AROI PERC [%]
10	1147.51	1687.45	114.75	168.75	2.14	3.79
12	2431.61	2876.20	202.63	235.6	3.79	5.29
15	4348.16	4635.06	289.88	309.00	5.42	6.93
20	7505.67	7502.94	375.28	375.15	7.01	8.42
30	13,711.93	13,008.04	457.06	433.60	8.54	9.73

For this 2.5 kW case, the PERC system would achieve the break-even point during the 8th year, while the HJT system would achieve the break-even point during the 9th year. After this time, they will turn into a lucrative investment. Similar to the 3.5 kW installation, in the long run, the HJT system will deliver more profits than the PERC system again despite the bigger investment costs and lower annual return on investment. During the 20th year, the HJT system will surpass the revenue of the PERC system.

6.4. Fixed Power Installations—Conclusions

After simulating 4.5 kW, 3.5 kW and 2.5 kW nominal power installations, it is possible to conclude the following:

- When comparing fixed power installations, it is possible to conclude through computations that a PERC system displays a better annual return on investment than an HJT system. This explains the reduced time that the PERC installation requires to achieve the break-even point;
- Despite displaying lower AROI, the HJT system will deliver more profit over time and will surpass the PERC system in the long run regarding profit;
- As the installed power decreases, the amount of time that the HJT installation requires to surpass the PERC installation profits increases. This happens due to the fixed installation costs. As less power is required, the number of photovoltaic modules decreases, and the costs related to the cables, inverter, labor and structures are more significant in comparison with the total investment costs;
- Likewise, when the installed power increases, the HJT installation will require less time to surpass the PERC installation profits;
- When there is an installation with power constraints or installation area, choosing a system composed of HJT modules will be more profitable.

### 6.5. EUR 5000 Investment Project

After performing three fixed power installations, two projects with fixed investment values were studied. The first one is considered an installation of EUR 5000. The same costs as the 4.5 kW project for cables, inverters, structures and labor were considered, as listed in Table 22. With the costs and the production of the systems computed, it is possible to see in Figure 37 the cumulative profits of these systems for 30 years. In Table 23, it is possible to observe the profits for years 12, 15, 20 and 30, as well as the APpY and AROI.

Table 22. HJT and PERC system costs for EUR 5000 installations.

Material	HJT [EUR]	PERC [EUR]
Modules	1356.93	1541.6
Inverters	1389.00	1314.99
Cables	280	280
Structure	781.82	781.82
Labor	1000	1000
Total	4807.75	4918.41

Table 23. Cumulative, APpY and AROI for 10, 12, 15, 20 and 30 years—EUR 5000 installation.

Years	HJT Profit [EUR]	PERC Profit [EUR]	APpY HJT [EUR]	APpY PERC [EUR]	AROI HJT [%]	AROI PERC [%]
10	−166.30	3857.84	−16.63	385.78	−0.35	7.84
12	750.91	5556.06	62.58	463.00	1.30	9.41
15	2119.88	8068.72	141.33	537.91	2.94	10.94
20	4375.24	12,165.68	218.76	608.28	4.55	12.37
30	8808.29	20,030.12	293.61	667.67	6.11	13.57
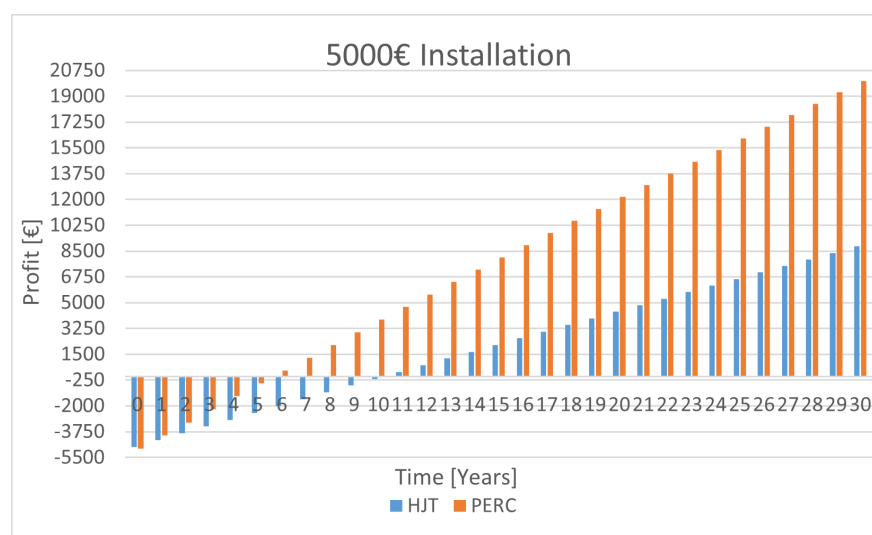
Figure 37. Cumulative profits of HJT and PERC systems over 30 years: EUR 5000 installation.

The results indicate that the PERC system would achieve the break-even point during the 6th year, while the HJT system would achieve the break-even point during the 11th year. After this time, they will turn into a lucrative investment. Unlike the fixed power installations, the PERC system displays much higher profits than the HJT installation and is never surpassed in profit. Throughout 30 years, the PERC system will display a much higher AROI than the HJT system.

6.6. EUR 10,000 Investment Project

One considers now an installation cost of EUR 10,000. Since the number of modules increased to 17 on HJT and 25 on PERC, new inverters are required for the HJT PV system and for the PERC PV system. The amount of cable increased by 50% on HJT and doubled on the PERC system. Regarding structures, both systems doubled these from the previous example. Labor costs also increased in the same proportion as cables. These new costs are listed in Table 24.

With the costs and the production of the systems computed, it is possible to verify in Figure 38 the cumulative profits of these systems over 30 years. In Table 25, it is possible to observe the profits for years 12, 15, 20 and 30, as well as the APpY and AROI.

Table 24. HJT and PERC system costs for EUR 10,000 installations.

Material	HJT [EUR]	PERC [EUR]
Modules	4613.55	3854
Inverters	1690	1970
Cables	420	560
Structure	1563.64	1563.64
Labor	1500	2000
Total	9787.19	9947.64

For a EUR 10,000 investment project, the results point to the PERC system achieving the break-even point during the 4th year, while the HJT system would achieve the break-even point during the 6th year. After this time, they will turn into a lucrative investment. Similar to the EUR 5000 installations, a big difference in profit and AROI benefits the PERC installation.
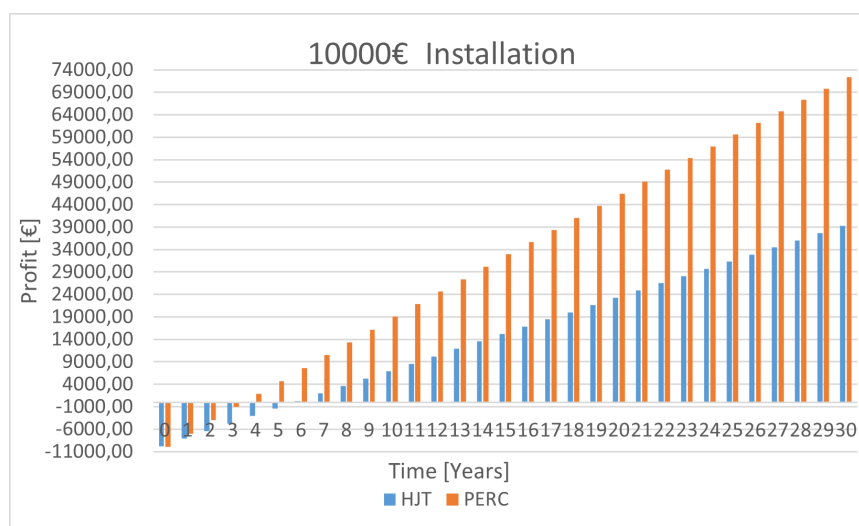
Figure 38. Cumulative profits of HJT and PERC systems over 30 years: EUR 10,000 installation.

Table 25. Cumulative, APpY and AROI for 10, 12, 15, 20 and 30 years—EUR 10000 installation.

Years	HJT Profit [EUR]	PERC Profit [EUR]	APpY HJT [EUR]	APpY PERC [EUR]	AROI HJT [%]	AROI PERC [%]
10	6922.02	19013.99	692.20	1901.40	7.07	19.11
12	10,223.98	24,618.12	852.00	2051.51	8.71	20.62
15	15,152.25	32,909.89	1010.15	2194.00	10.3	22.01
20	23,271.57	46,429.87	1163.58	2321.49	11.89	23.33
30	39,230.53	72,382.51	1307.68	2412.75	13.36	24.25

6.7. Fixed Investment Installations—Conclusions

After analyzing the cases of EUR 5000 and EUR 10,000 installations, it is possible to conclude the following:

- The PERC system will return more profit in comparison with the HJT installation;
- The PERC system displays much higher AROI than the HJT system;
- When the budget of the installations increased from EUR 5000 to EUR 10,000, both installations suffered components updates. Despite this, since the PERC modules are cheaper, an increased budget reflects a bigger increase in the number of modules compared to the HJT system. This way, the remaining system components suffered a bigger intervention on the PERC system. This explains the smaller visual difference in the profits on the EUR 10,000 system, visualized in Figure 38, in comparison to the EUR 5000 system, visualized in Figure 37.
- When there is an installation with investment constraints, choosing a system composed of PERC modules is a better investment.

6.8. HJT and PERC Modules Malfunction and Replacement

Five projects have already been studied for 30 years. It is important to note that the PERC modules only display 12 years of product warranty. If modules stop working from year 13, *JAsolar* will not replace these devices. Since the HJT modules display 30 years of product warranty, it is also important to compute a situation where PERC modules fail outside of the warranty. As HJT modules displayed better economic performance with fixed power installations and the warranty discussion will only influence the PERC modules if there is failure in under 30 years, it will be interesting to compare the fixed investment installations to understand if the PERC modules, if replaced, are still a better investment option than the HJT modules.

The EUR 10,000 installations will be analyzed in this section. Various simulations were performed, from replacing 10% of the modules to replacing 100% of them. Since there was no displayed major difference until there was a need to replace 100% of the modules, the worst-case scenario will be displayed. The whole number of modules, 25, will need replacement every 12 years. EUR 1500 of labor was considered for the two necessary replacements in years 13 and 25. Twenty-five modules account for a total of EUR 3854.

Figure 39 displays the new cumulative profits. It is possible to conclude that, even in the worst-case scenario, for a EUR 10,000 installation, PERC is the technology that should be chosen to perform fixed investment installations.

Now, the same situation applies to the EUR 5000 installations. Ten modules will be replaced in years 13 and 25, costing EUR 1541 in modules and EUR 1000 in labor for each intervention. The new cumulative profits are displayed in Figure 40. It is possible to conclude that, even in the worst-case scenario, for a EUR 5000 installation, PERC is the technology that should be chosen to perform fixed investment installations.
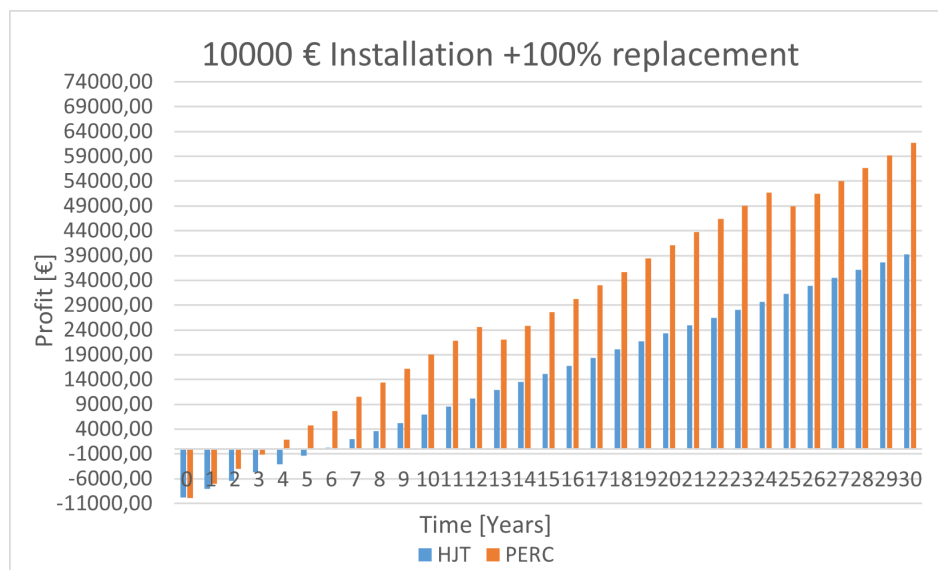
Figure 39. Cumulative profits of HJT and PERC systems over 30 years: EUR 10.000 installation with module replacements in years 13 and 25.
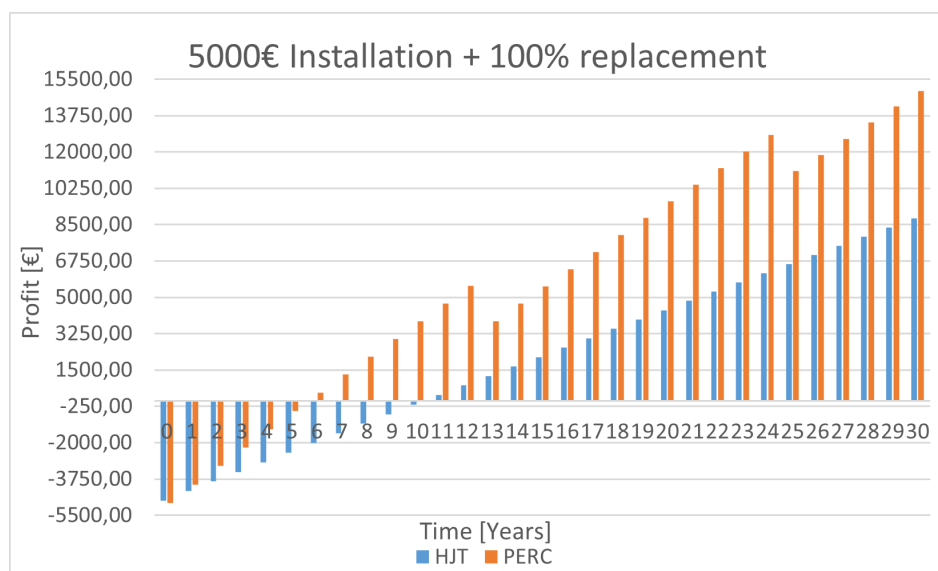
Figure 40. Cumulative profits of HJT and PERC systems over 30 years: EUR 5.000 installation with module replacements in years 13 and 25.

7. Conclusions

The HJT module had outperformed the PERC module in conditions where irradiance surpassed the 300 W/m^2 value by an average of 1.88%. In the presence of clouds, the PERC module displayed better efficiency, but, analyzing that both modules output low power due to the lack of irradiance, this difference can be neglected.

After collecting data that characterize module behavior, it was possible to simulate the performance of some installations and compare the economic performance. It was concluded that, in the presence of installations with constraints of installed power or installation area, it is better to choose the HJT technology for these projects. As the nominal power will be similar, the more expensive and more efficient HJT modules will turn more profitable in the long run, despite both installations achieving the break-even point considerably fast, making them good investments.

When projects have limited investment, PERC is the technology that should be used in the installations. The lower costs of the modules allow for more modules to be installed,

which will compensate for the slightly lower efficiency displayed in the experimental analysis. For this type of installation, even considering the worst-case scenario where the PERC modules need to be replaced as soon as the warranty expires, it was concluded that they were still the viable solution to search for.

Although experimental analysis has been performed and conclusions about the performance of two technologies were given, there is still some future work that can be carried out:

- Installation of the modules oriented directly toward the sun to optimize exposure and increase output power, and the HJT module can receive irradiance from both sides, increasing its efficiency;
- Installation of two modules of each technology in which one of the modules does not receive any cleaning to understand and compare the performance of these effects on the output;
- Comparison of HJT technology with other technologies that have been raising interest over the last years, such as interdigitated back contact (IBC) cells and tunnel oxide passivated contact (TOPcon) cells;
- Introduction of cooling techniques to understand the effect of temperature in a module with the same irradiance, and study of the economic feasibility of these new projects.

Author Contributions: Methodology, A.S.; Validation, A.S.; Investigation, A.S.; Writing—original draft, A.S.; Writing—review & editing, P.B.; Supervision, P.B. All authors have read and agreed to the published version of the manuscript.

Data Availability Statement: The original contributions presented in the study are included in the article, further inquiries can be directed to the corresponding author/s.

Conflicts of Interest: The authors declare no conflict of interest.

References

1. IEA PVPS. Photovoltaic Power Systems Programme Annual Report 2020. Technical Report, IEA PVPS. 2020. Available online: https://iea-pvps.org/wp-content/uploads/2021/04/IEA-PVPS-AR-2020.pdf (accessed on 16 July 2020).
2. Wang, Q.; Guo, K.; Gu, S.; Huang, W.; Peng, H.; Wu, W.; Ding, J. Electrical Performance, Loss Analysis, and Efficiency Potential of Industrial-Type PERC, TOPCon, and SHJ Solar Cells: A Comparative Study. *Prog. Photovolt. Res. Appl.* **2024**, *32*, 3839–3852. [CrossRef]
3. Li, M.; Zhang, W.; Chen, Y.; Liu, J.; Wang, L.; Huang, X. Energy yield analysis of different bifacial PV (photovoltaic) technologies: TOPCon, HJT, PERC in Hainan. *Renew. Energy* **2024**, *85*, 1234–1245. [CrossRef]
4. Smith, J.; Doe, J.; Brown, E.; Johnson, M. Review of Mono- and Bifacial Photovoltaic Technologies: A Comparative Study. *Solar Energy Mater. Sol. Cells* **2024**, *95*, 3456–3467. [CrossRef]
5. Johnson, M.; Lee, S.; Kim, D.; Chen, L. Performance assessment of a bifacial PV system using a new energy estimation model. *J. Renew. Energy* **2024**, *78*, 567–578. [CrossRef]
6. Maniscalco, M.P.; Longo, S.; Miccichè, G.; Cellura, M.; Ferraro, M. A Critical Review of the Environmental Performance of Bifacial Photovoltaic Panels. *Energies* **2024**, *17*, 226. [CrossRef]
7. Hezel, R.; Jaeger, K. Low-temperature surface passivation of silicon for solar cells. *J. Electrochem. Soc.* **1989**, *136*, 518. [CrossRef]
8. Jaeger, K.; Hezel, R. A novel thin silicon solar cell with Al_2O_3 as surface passivation. In Proceedings of the IEEE Photovoltaic Specialists Conference, 18, Las Vegas, NV, USA, 21–25 October 1985; pp. 1752–1753.
9. Schmidt, J.; Werner, F.; Veith, B.; Zielke, D.; Steingrube, S.; Altermatt, P.P.; Gatz, S.; Dullweber, T.; Brendel, R. Advances in the surface passivation of silicon solar cells. *Energy Procedia* **2012**, *15*, 30–39. [CrossRef]
10. Kray, D.; Hermle, M.; Glunz, S.W. Theory and experiments on the back side reflectance of silicon wafer solar cells. *Prog. Photovolt. Res. Appl.* **2008**, *16*, 1–15. [CrossRef]
11. Lotsch, H.K.V. *High Efficient Low Cost Photvoltaics: Recent Developments*; Springer: Berlin/Heidelberg, Germany, 2020; p. 110.
12. Mikolášek, M. Silicon Heterojunction Solar Cells: The Key Role of Heterointerfaces and their Impact on the Performance. In *Nanostructured Solar Cells*; Das, N., Ed.; IntechOpen: Rijeka, Croatia, 2017; Chapter 4. [CrossRef]

13. Hoex, B.; Heil, S.; Langereis, E.; Van de Sanden, M.; Kessels, W. Ultralow surface recombination of c-Si substrates passivated by plasma-assisted atomic layer deposited Al_2O_3. *Appl. Phys. Lett.* **2006**, *89*, 042112. [CrossRef]

14. Chen, D.; Vaqueiro Contreras, M.; Ciesla, A.; Hallam, B.; Abbott, M.; Chan, C. Research progress of light and elevated temperature-induced degradation in silicon solar cells: A review. *Prog. Photovolt. Res. Appl.* **2024**, *32*, 4567–4582. [CrossRef]

15. Söderström, T.; Papet, P.; Ufheil, J. Smart wire connection technology. In Proceedings of the the 28th European Photovoltaic Solar Energy Conference, Paris, France, 30 September–4 October 2013; pp. 495–499.

16. Smith, J.; Lee, S.; Kim, D.; Chen, L. Illumination-dependent temperature coefficients of the electrical parameters of modern silicon solar cell architectures. *Sol. Energy* **2024**, *210*, 123–134. [CrossRef]

17. Lopez-Garcia, J.; Gracia-Amillo, A.; Urraca-Valle, R.; Kenny, R.P.; Sample, T. Analysis of temperature coefficients of bifacial crystalline silicon PV modules. *IEEE J. Photovolt.* **2024**, *8*, 968–975. [CrossRef]

18. Schneider, A.; Chochollek, J.; Nierhoff, T. Advanced Determination of Temperature Coefficients of Photovoltaic Modules by Field Measurements. In Proceedings of the SiliconPV 2023, 13th International Conference on Crystalline Silicon Photovoltaics Module Reliability and Energy Yield, Delft, The Netherlands & Online, 11–14 April 2023. [CrossRef]

19. Cortés, B.; Tapia, R.; Flores, J.J. System-Independent Irradiance Sensorless ANN-Based MPPT for Photovoltaic Systems in Electric Vehicles. *Energies* **2021**, *14*, 4820. [CrossRef]

20. Gupta, A.K.; Pachauri, R.K.; Maity, T.; Chauhan, Y.K.; Mahela, O.P.; Khan, B.; Gupta, P.K. Effect of Various Incremental Conductance MPPT Methods on the Charging of Battery Load Feed by Solar Panel. *IEEE Access* **2021**, *9*, 12345–12356. [CrossRef]

21. Logothetis, S.A.; Salamalikis, V.; Nouri, B.; Remund, J.; Zarzalejo, L.F.; Xie, Y.; Wilbert, S.; Ntavelis, E.; Nou, J.; Hendrikx, N.; et al. Solar irradiance ramp forecasting based on all-sky imagers. *Energies* **2022**, *15*, 6191. [CrossRef]

22. Sahin, G.; Isik, G.; van Sark, W.G. Predictive modeling of PV solar power plant efficiency considering weather conditions: A comparative analysis of artificial neural networks and multiple linear regression. *Energy Rep.* **2023**, *10*, 2837–2849. [CrossRef]

23. Nelega, R.; Greu, D.I.; Jecan, E.; Rednic, V.; Zamfirescu, C.; Puschita, E.; Turcu, R.V.F. Prediction of power generation of a photovoltaic power plant based on neural networks. *IEEE Access* **2023**, *11*, 12345–12356. [CrossRef]

24. Tehrani, A.A.; Veisi, O.; Fakhr, B.V.; Du, D. Predicting solar radiation in the urban area: A data-driven analysis for sustainable city planning using artificial neural networking. *Sustain. Cities Soc.* **2024**, *100*, 105042. [CrossRef]

25. Santos, L.d.O.; Carvalho, P.C.M.d.; Carvalho Filho, C.d.O. Photovoltaic cell operating temperature models: A review of correlations and parameters. *IEEE J. Photovolt.* **2022**, *12*, 179–190. [CrossRef]

26. European Commission, Joint Research Centre. Photovoltaic Geographical Information System (PVGIS). *European Commission*. 2024. Available online: https://ec.europa.eu/jrc/en/pvgis (accessed on 8 May 2020).

27. Fronius International GmbH. Fronius Primo 4.0-1. *Fronius International GmbH*. 2024. Available online: https://www.fronius.com/en-gb/uk/solar-energy/installers-partners/technical-data/all-products/inverters/fronius-primo/fronius-primo-4-0-1 (accessed on 13 July 2020).

28. Fronius International GmbH. Fronius Primo 3.5-1. *Fronius International GmbH*. 2024. Available online: https://www.fronius.com/~/downloads/Solar%20Energy/Datasheets/SE_DS_Fronius_Primo_EN.pdf (accessed on 13 July 2020).